Chapter 9 Phase Diagrams

The graph below is the phase diagram for pure H_2O. Parameters plotted are external pressure (vertical axis, scaled logarithmically) versus temperature. In a sense this diagram is a map wherein regions for the three familiar phases—solid (ice), liquid (water), and vapor (steam)—are delineated. The three red curves represent phase boundaries that define the regions. A photograph located in each region shows an example of its phase—ice cubes, liquid water being poured into a glass, and steam that is spewing forth from a kettle. (Photographs courtesy of iStockphoto.)

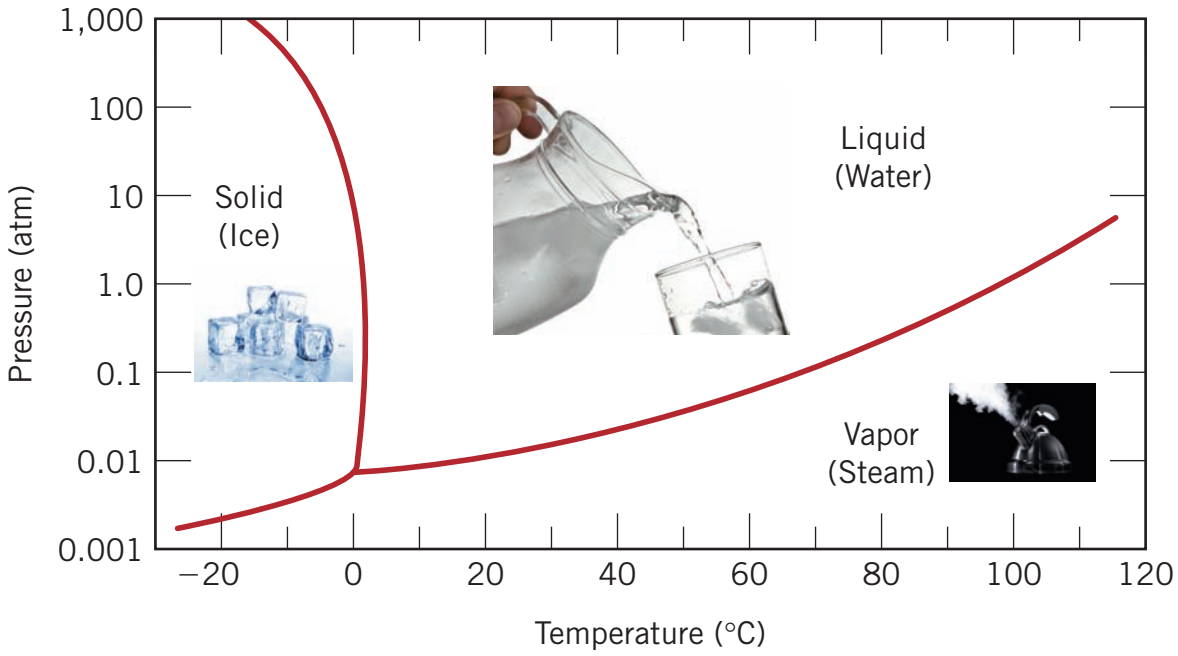

WHY STUDY *Phase Diagrams?*

One reason that a knowledge and understanding of phase diagrams is important to the engineer relates to the design and control of heat-treating procedures; some properties of materials are functions of their microstructures, and, consequently, of their thermal histories. Even though most phase diagrams represent stable (or equilibrium) states and microstructures, they are nevertheless useful in understanding the development and preservation of nonequilibrium structures and their attendant properties; it is often the case that these properties are more desirable than those associated with the equilibrium state. This is aptly illustrated by the phenomenon of precipitation hardening (Section 11.9).

In the processing/structure/properties/performance scheme, reasons for studying phase diagrams are as follows:

- Concepts discussed in this chapter provide a foundation that is necessary for us to understand phase transformations that occur in steel alloys, as well as the consequences of these transformations—that is, microstructural and property alterations (as presented in Chapter 10).

Learning Objectives

After studying this chapter you should be able to do the following:

1. (a) Schematically sketch simple isomorphous and eutectic phase diagrams.
   (b) On these diagrams label the various phase regions.
   (c) Label liquidus, solidus, and solvus lines.
2. Given a binary phase diagram, the composition of an alloy, its temperature, and assuming that the alloy is at equilibrium, determine
   (a) what phase(s) is (are) present,
   (b) the composition(s) of the phase(s), and
   (c) the mass fraction(s) of the phase(s).
3. For some given binary phase diagram, do the following:
   (a) locate the temperatures and compositions of all eutectic, eutectoid, peritectic, and congruent phase transformations; and
   (b) write reactions for all these transformations for either heating or cooling.
4. Given the composition of an iron–carbon alloy containing between 0.022 wt% C and 2.14 wt% C, be able to
   (a) specify whether the alloy is hypoeutectoid or hypereutectoid,
   (b) name the proeutectoid phase,
   (c) compute the mass fractions of proeutectoid phase and pearlite, and
   (d) make a schematic diagram of the microstructure at a temperature just below the eutectoid.

9.1 INTRODUCTION

The understanding of phase diagrams for alloy systems is extremely important because there is a strong correlation between microstructure and mechanical properties, and the development of microstructure of an alloy is related to the characteristics of its phase diagram. In addition, phase diagrams provide valuable information about melting, casting, crystallization, and other phenomena.

This chapter presents and discusses the following topics: (1) terminology associated with phase diagrams and phase transformations; (2) pressure–temperature phase diagrams for pure materials; (3) the interpretation of phase diagrams; (4) some of the common and relatively simple binary phase diagrams, including that for the iron–carbon system; and (5) the development of equilibrium microstructures, upon cooling, for several situations.

Definitions and Basic Concepts

component

It is necessary to establish a foundation of definitions and basic concepts relating to alloys, phases, and equilibrium before delving into the interpretation and utilization of phase diagrams. The term **component** is frequently used in this discussion; components are pure metals and/or compounds of which an alloy is composed. For example, in a copper–zinc brass, the components are Cu and Zn. *Solute* and *solvent,* which are also common terms, were defined in Section 4.3. Another term used in this context is **system,** which has two meanings. First, *system* may refer to a specific body of material under consideration (e.g., a ladle of molten steel). Or it may relate to the series of possible alloys consisting of the same components, but without regard to alloy composition (e.g., the iron–carbon system).

system

The concept of a solid solution was introduced in Section 4.3. By way of review, a solid solution consists of atoms of at least two different types; the solute atoms occupy either substitutional or interstitial positions in the solvent lattice, and the crystal structure of the solvent is maintained.

9.2 SOLUBILITY LIMIT

solubility limit

For many alloy systems and at some specific temperature, there is a maximum concentration of solute atoms that may dissolve in the solvent to form a solid solution; this is called a **solubility limit.** The addition of solute in excess of this solubility limit results in the formation of another solid solution or compound that has a distinctly different composition. To illustrate this concept, consider the sugar–water ($C_{12}H_{22}O_{11}$–H_2O) system. Initially, as sugar is added to water, a sugar–water solution or syrup forms. As more sugar is introduced, the solution becomes more concentrated, until the solubility limit is reached or the solution becomes saturated with sugar. At this time the solution is not capable of dissolving any more sugar, and further additions simply settle to the bottom of the container. Thus, the system now consists of two separate substances: a sugar–water syrup liquid solution and solid crystals of undissolved sugar.

This solubility limit of sugar in water depends on the temperature of the water and may be represented in graphical form on a plot of temperature along the ordinate and composition (in weight percent sugar) along the abscissa, as shown in Figure 9.1. Along the composition axis, increasing sugar concentration is from left to right, and percentage of water is read from right to left. Because only two

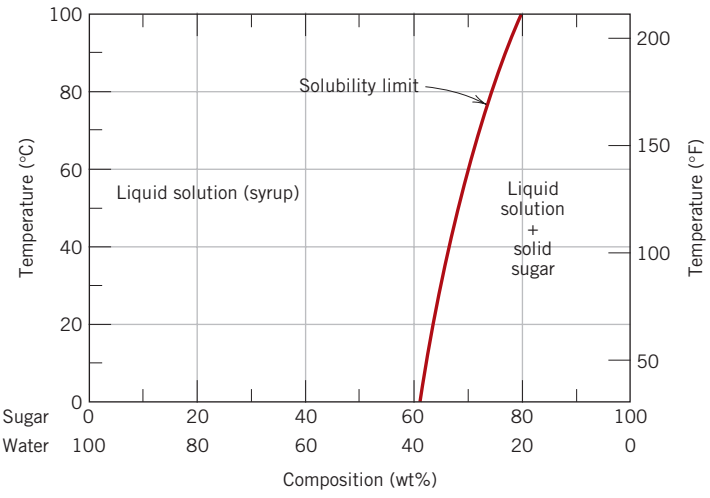

Figure 9.1 The solubility of sugar ($C_{12}H_{22}O_{11}$) in a sugar–water syrup.

components are involved (sugar and water), the sum of the concentrations at any composition will equal 100 wt%. The solubility limit is represented as the nearly vertical line in the figure. For compositions and temperatures to the left of the solubility line, only the syrup liquid solution exists; to the right of the line, syrup and solid sugar coexist. The solubility limit at some temperature is the composition that corresponds to the intersection of the given temperature coordinate and the solubility limit line. For example, at 20°C the maximum solubility of sugar in water is 65 wt%. As Figure 9.1 indicates, the solubility limit increases slightly with rising temperature.

9.3 PHASES

phase

Also critical to the understanding of phase diagrams is the concept of a **phase.** A phase may be defined as a homogeneous portion of a system that has uniform physical and chemical characteristics. Every pure material is considered to be a phase; so also is every solid, liquid, and gaseous solution. For example, the sugar–water syrup solution just discussed is one phase, and solid sugar is another. Each has different physical properties (one is a liquid, the other is a solid); furthermore, each is different chemically (i.e., has a different chemical composition); one is virtually pure sugar, the other is a solution of H_2O and $C_{12}H_{22}O_{11}$. If more than one phase is present in a given system, each will have its own distinct properties, and a boundary separating the phases will exist across which there will be a discontinuous and abrupt change in physical and/or chemical characteristics. When two phases are present in a system, it is not necessary that there be a difference in both physical and chemical properties; a disparity in one or the other set of properties is sufficient. When water and ice are present in a container, two separate phases exist; they are physically dissimilar (one is a solid, the other is a liquid) but identical in chemical makeup. Also, when a substance can exist in two or more polymorphic forms (e.g., having both FCC and BCC structures), each of these structures is a separate phase because their respective physical characteristics differ.

Sometimes, a single-phase system is termed *homogeneous*. Systems composed of two or more phases are termed *mixtures* or *heterogeneous systems*. Most metallic alloys and, for that matter, ceramic, polymeric, and composite systems are heterogeneous. Ordinarily, the phases interact in such a way that the property combination of the multiphase system is different from, and more attractive than, either of the individual phases.

9.4 MICROSTRUCTURE

Many times, the physical properties and, in particular, the mechanical behavior of a material depend on the microstructure. Microstructure is subject to direct microscopic observation, using optical or electron microscopes; this topic was touched on in Sections 4.9 and 4.10. In metal alloys, microstructure is characterized by the number of phases present, their proportions, and the manner in which they are distributed or arranged. The microstructure of an alloy depends on such variables as the alloying elements present, their concentrations, and the heat treatment of the alloy (i.e., the temperature, the heating time at temperature, and the rate of cooling to room temperature).

The procedure of specimen preparation for microscopic examination was briefly outlined in Section 4.10. After appropriate polishing and etching, the different phases may be distinguished by their appearance. For example, for a two-phase

alloy, one phase may appear light and the other phase dark. When only a single phase or solid solution is present, the texture will be uniform, except for grain boundaries that may be revealed (Figure 4.14*b*).

9.5 PHASE EQUILIBRIA

equilibrium

free energy

Equilibrium is another essential concept that is best described in terms of a thermodynamic quantity called the **free energy.** In brief, free energy is a function of the internal energy of a system, and also the randomness or disorder of the atoms or molecules (or entropy). A system is at equilibrium if its free energy is at a minimum under some specified combination of temperature, pressure, and composition. In a macroscopic sense, this means that the characteristics of the system do not change with time but persist indefinitely; that is, the system is stable. A change in temperature, pressure, and/or composition for a system in equilibrium will result in an increase in the free energy and in a possible spontaneous change to another state whereby the free energy is lowered.

phase equilibrium

The term **phase equilibrium,** often used in the context of this discussion, refers to equilibrium as it applies to systems in which more than one phase may exist. Phase equilibrium is reflected by a constancy with time in the phase characteristics of a system. Perhaps an example best illustrates this concept. Suppose that a sugar–water syrup is contained in a closed vessel and the solution is in contact with solid sugar at 20°C. If the system is at equilibrium, the composition of the syrup is 65 wt% $C_{12}H_{22}O_{11}$–35 wt% H_2O (Figure 9.1), and the amounts and compositions of the syrup and solid sugar will remain constant with time. If the temperature of the system is suddenly raised—say, to 100°C—this equilibrium or balance is temporarily upset in that the solubility limit has been increased to 80 wt% $C_{12}H_{22}O_{11}$ (Figure 9.1). Thus, some of the solid sugar will go into solution in the syrup. This will continue until the new equilibrium syrup concentration is established at the higher temperature.

This sugar–syrup example illustrates the principle of phase equilibrium using a liquid–solid system. In many metallurgical and materials systems of interest, phase equilibrium involves just solid phases. In this regard the state of the system is reflected in the characteristics of the microstructure, which necessarily include not only the phases present and their compositions but, in addition, the relative phase amounts and their spatial arrangement or distribution.

Free energy considerations and diagrams similar to Figure 9.1 provide information about the equilibrium characteristics of a particular system, which is important, but they do not indicate the time period necessary for the attainment of a new equilibrium state. It is often the case, especially in solid systems, that a state of equilibrium is never completely achieved because the rate of approach to equilibrium is extremely slow; such a system is said to be in a nonequilibrium or **metastable** state. A metastable state or microstructure may persist indefinitely, experiencing only extremely slight and almost imperceptible changes as time progresses. Often, metastable structures are of more practical significance than equilibrium ones. For example, some steel and aluminum alloys rely for their strength on the development of metastable microstructures during carefully designed heat treatments (Sections 10.5 and 11.9).

metastable

Thus not only is an understanding of equilibrium states and structures important, but also the speed or rate at which they are established and the factors that affect the rate must be considered. This chapter is devoted almost exclusively to equilibrium structures; the treatment of reaction rates and nonequilibrium structures is deferred to Chapter 10 and Section 11.9.

Concept Check 9.1

What is the difference between the states of phase equilibrium and metastability?

[*The answer may be found at www.wiley.com/college/callister (Student Companion Site).*]

9.6 ONE-COMPONENT (OR UNARY) PHASE DIAGRAMS

phase diagram

Much of the information about the control of the phase structure of a particular system is conveniently and concisely displayed in what is called a **phase diagram,** also often termed an *equilibrium diagram.* Now, there are three externally controllable parameters that will affect phase structure—temperature, pressure, and composition—and phase diagrams are constructed when various combinations of these parameters are plotted against one another.

Perhaps the simplest and easiest type of phase diagram to understand is that for a one-component system, in which composition is held constant (i.e., the phase diagram is for a pure substance); this means that pressure and temperature are the variables. This one-component phase diagram (or *unary phase diagram*) [sometimes also called a *pressure–temperature* (or *P–T*) *diagram*] is represented as a two-dimensional plot of pressure (ordinate, or vertical axis) versus temperature (abscissa, or horizontal axis). Most often, the pressure axis is scaled logarithmically.

We illustrate this type of phase diagram and demonstrate its interpretation using as an example the one for H_2O, which is shown in Figure 9.2. Here it may be noted that regions for three different phases—solid, liquid, and vapor—are delineated on the plot. Each of the phases will exist under equilibrium conditions over the temperature–pressure ranges of its corresponding area. Furthermore, the three curves shown on the plot (labeled *aO*, *bO*, and *cO*) are phase boundaries; at any point on one of these curves, the two phases on either side of the curve are in equilibrium (or coexist) with one another. That is, equilibrium between solid and vapor

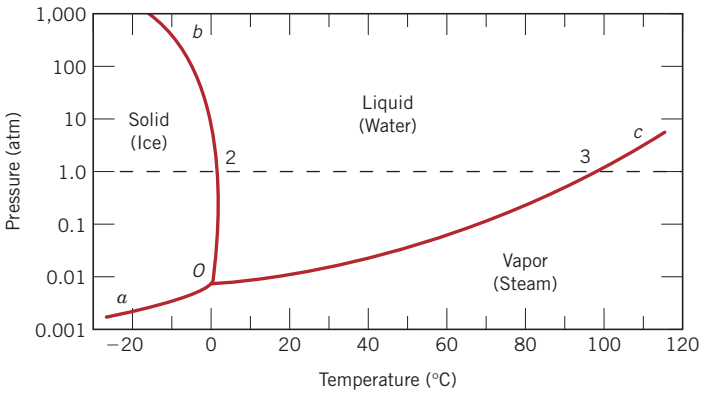

Figure 9.2 Pressure–temperature phase diagram for H_2O. Intersection of the dashed horizontal line at 1 atm pressure with the solid–liquid phase boundary (point 2) corresponds to the melting point at this pressure ($T = 0°C$). Similarly, point 3, the intersection with the liquid–vapor boundary, represents the boiling point ($T = 100°C$).

phases is along curve *aO*—likewise for the solid–liquid, curve *bO*, and the liquid–vapor, curve *cO*. Also, upon crossing a boundary (as temperature and/or pressure is altered), one phase transforms to another. For example, at 1 atm pressure, during heating the solid phase transforms to the liquid phase (i.e., melting occurs) at the point labeled 2 on Figure 9.2 (i.e., the intersection of the dashed horizontal line with the solid–liquid phase boundary); this point corresponds to a temperature of 0°C. Of course, the reverse transformation (liquid-to-solid, or solidification) takes place at the same point upon cooling. Similarly, at the intersection of the dashed line with the liquid–vapor phase boundary [point 3 (Figure 9.2), at 100°C] the liquid transforms to the vapor phase (or vaporizes) upon heating; condensation occurs for cooling. And, finally, solid ice sublimes or vaporizes upon crossing the curve labeled *aO*.

As may also be noted from Figure 9.2, all three of the phase boundary curves intersect at a common point, which is labeled *O* (and for this H_2O system, at a temperature of 273.16 K and a pressure of 6.04×10^{-3} atm). This means that at this point only, all of the solid, liquid, and vapor phases are simultaneously in equilibrium with one another. Appropriately, this, and any other point on a *P*–*T* phase diagram where three phases are in equilibrium, is called a *triple point;* sometimes it is also termed an *invariant point* inasmuch as its position is distinct, or fixed by definite values of pressure and temperature. Any deviation from this point by a change of temperature and/or pressure will cause at least one of the phases to disappear.

Pressure–temperature phase diagrams for a number of substances have been determined experimentally, which also have solid, liquid, and vapor phase regions. In those instances when multiple solid phases (i.e., allotropes, Section 3.6) exist, there will appear a region on the diagram for each solid phase, and also other triple points.

Binary Phase Diagrams

Another type of extremely common phase diagram is one in which temperature and composition are variable parameters, and pressure is held constant—normally 1 atm. There are several different varieties; in the present discussion, we will concern ourselves with binary alloys—those that contain two components. If more than two components are present, phase diagrams become extremely complicated and difficult to represent. An explanation of the principles governing and the interpretation of phase diagrams can be demonstrated using binary alloys even though most alloys contain more than two components.

Binary phase diagrams are maps that represent the relationships between temperature and the compositions and quantities of phases at equilibrium, which influence the microstructure of an alloy. Many microstructures develop from phase transformations, the changes that occur when the temperature is altered (ordinarily upon cooling). This may involve the transition from one phase to another, or the appearance or disappearance of a phase. Binary phase diagrams are helpful in predicting phase transformations and the resulting microstructures, which may have equilibrium or nonequilibrium character.

9.7 BINARY ISOMORPHOUS SYSTEMS

Possibly the easiest type of binary phase diagram to understand and interpret is the type that is characterized by the copper–nickel system (Figure 9.3*a*). Temperature is plotted along the ordinate, and the abscissa represents the composition of the alloy, in weight percent (bottom) and atom percent (top) of nickel. The composition

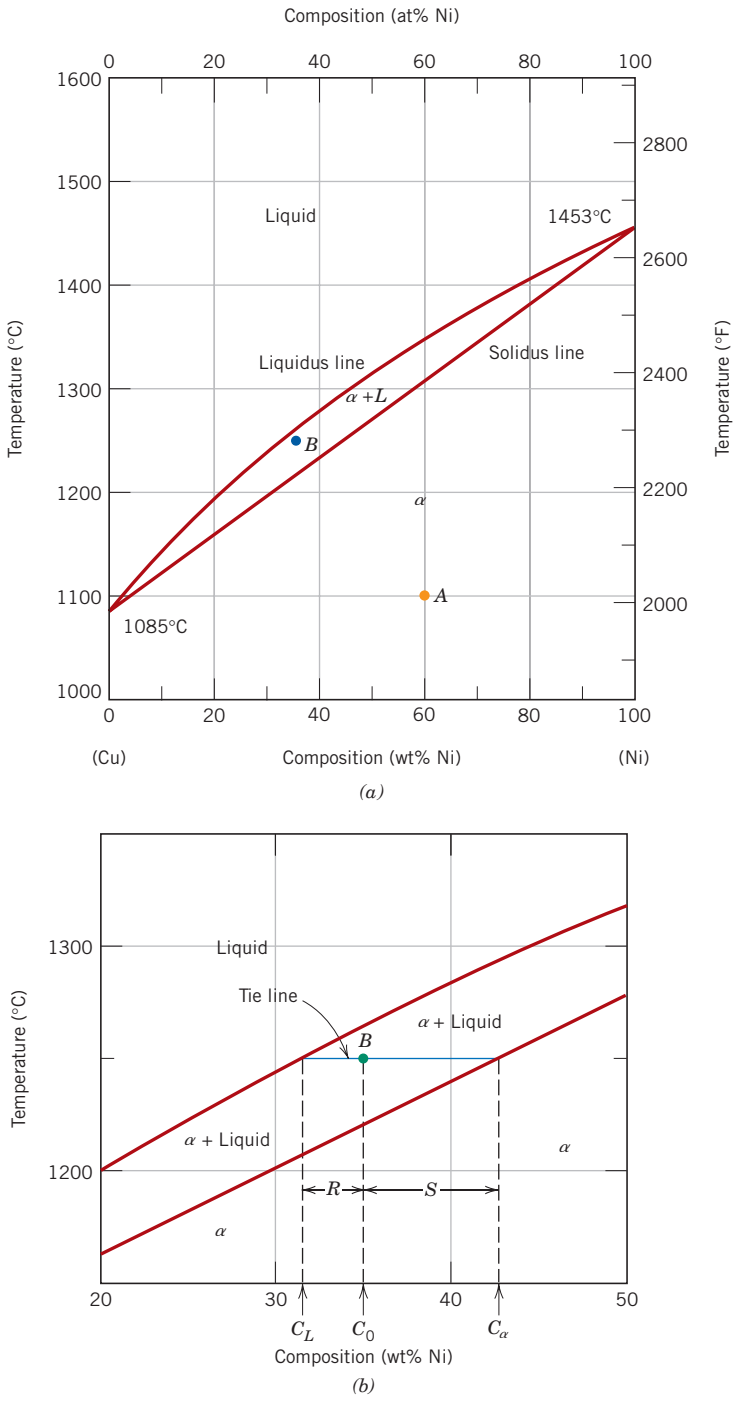

Figure 9.3 (*a*) The copper–nickel phase diagram. (*b*) A portion of the copper–nickel phase diagram for which compositions and phase amounts are determined at point *B*. (Adapted from *Phase Diagrams of Binary Nickel Alloys*, P. Nash, Editor, 1991. Reprinted by permission of ASM International, Materials Park, OH.)

ranges from 0 wt% Ni (100 wt% Cu) on the left horizontal extremity to 100 wt% Ni (0 wt% Cu) on the right. Three different phase regions, or fields, appear on the diagram, an alpha (α) field, a liquid (L) field, and a two-phase $\alpha + L$ field. Each region is defined by the phase or phases that exist over the range of temperatures and compositions delineated by the phase boundary lines.

The liquid L is a homogeneous liquid solution composed of both copper and nickel. The α phase is a substitutional solid solution consisting of both Cu and Ni atoms, and having an FCC crystal structure. At temperatures below about 1080°C, copper and nickel are mutually soluble in each other in the solid state for all compositions. This complete solubility is explained by the fact that both Cu and Ni have the same crystal structure (FCC), nearly identical atomic radii and electronegativities, and similar valences, as discussed in Section 4.3. The copper–nickel system is termed **isomorphous** because of this complete liquid and solid solubility of the two components.

isomorphous

A couple of comments are in order regarding nomenclature. First, for metallic alloys, solid solutions are commonly designated by lowercase Greek letters (α, β, γ, etc.). Furthermore, with regard to phase boundaries, the line separating the L and $\alpha + L$ phase fields is termed the *liquidus line,* as indicated in Figure 9.3*a*; the liquid phase is present at all temperatures and compositions above this line. The *solidus line* is located between the α and $\alpha + L$ regions, below which only the solid α phase exists.

For Figure 9.3*a*, the solidus and liquidus lines intersect at the two composition extremities; these correspond to the melting temperatures of the pure components. For example, the melting temperatures of pure copper and nickel are 1085°C and 1453°C, respectively. Heating pure copper corresponds to moving vertically up the left-hand temperature axis. Copper remains solid until its melting temperature is reached. The solid-to-liquid transformation takes place at the melting temperature, and no further heating is possible until this transformation has been completed.

For any composition other than pure components, this melting phenomenon will occur over the range of temperatures between the solidus and liquidus lines; both solid α and liquid phases will be in equilibrium within this temperature range. For example, upon heating an alloy of composition 50 wt% Ni–50 wt% Cu (Figure 9.3*a*), melting begins at approximately 1280°C (2340°F); the amount of liquid phase continuously increases with temperature until about 1320°C (2410°F), at which the alloy is completely liquid.

9.8 INTERPRETATION OF PHASE DIAGRAMS

For a binary system of known composition and temperature that is at equilibrium, at least three kinds of information are available: (1) the phases that are present, (2) the compositions of these phases, and (3) the percentages or fractions of the phases. The procedures for making these determinations will be demonstrated using the copper–nickel system.

Phases Present

VMSE

Isomorphous (Sb-Bi)

The establishment of what phases are present is relatively simple. One just locates the temperature–composition point on the diagram and notes the phase(s) with which the corresponding phase field is labeled. For example, an alloy of composition 60 wt% Ni–40 wt% Cu at 1100°C would be located at point A in Figure 9.3*a*; because this is within the α region, only the single α phase will be present. On the other hand, a 35 wt% Ni–65 wt% Cu alloy at 1250°C (point B) will consist of both α and liquid phases at equilibrium.

Determination of Phase Compositions

The first step in the determination of phase compositions (in terms of the concentrations of the components) is to locate the temperature–composition point on the

VMSE

Isomorphous (Sb-Bi)

phase diagram. Different methods are used for single- and two-phase regions. If only one phase is present, the procedure is trivial: the composition of this phase is simply the same as the overall composition of the alloy. For example, consider the 60 wt% Ni–40 wt% Cu alloy at 1100°C (point *A*, Figure 9.3*a*). At this composition and temperature, only the α phase is present, having a composition of 60 wt% Ni–40 wt% Cu.

For an alloy having composition and temperature located in a two-phase region, the situation is more complicated. In all two-phase regions (and in two-phase regions only), one may imagine a series of horizontal lines, one at every temperature; each of these is known as a **tie line,** or sometimes as an isotherm. These tie lines extend across the two-phase region and terminate at the phase boundary lines on either side. To compute the equilibrium concentrations of the two phases, the following procedure is used:

tie line

1. A tie line is constructed across the two-phase region at the temperature of the alloy.
2. The intersections of the tie line and the phase boundaries on either side are noted.
3. Perpendiculars are dropped from these intersections to the horizontal composition axis, from which the composition of each of the respective phases is read.

For example, consider again the 35 wt% Ni–65 wt% Cu alloy at 1250°C, located at point *B* in Figure 9.3*b* and lying within the $\alpha + L$ region. Thus, the problem is to determine the composition (in wt% Ni and Cu) for both the α and liquid phases. The tie line has been constructed across the $\alpha + L$ phase region, as shown in Figure 9.3*b*. The perpendicular from the intersection of the tie line with the liquidus boundary meets the composition axis at 31.5 wt% Ni–68.5 wt% Cu, which is the composition of the liquid phase, C_L. Likewise, for the solidus–tie line intersection, we find a composition for the α solid-solution phase, C_α, of 42.5 wt% Ni–57.5 wt% Cu.

Determination of Phase Amounts

VMSE

Isomorphous (Sb-Bi)

The relative amounts (as fraction or as percentage) of the phases present at equilibrium may also be computed with the aid of phase diagrams. Again, the single- and two-phase situations must be treated separately. The solution is obvious in the single-phase region: because only one phase is present, the alloy is composed entirely of that phase; that is, the phase fraction is 1.0 or, alternatively, the percentage is 100%. From the previous example for the 60 wt% Ni–40 wt% Cu alloy at 1100°C (point *A* in Figure 9.3*a*), only the α phase is present; hence, the alloy is completely or 100% α.

If the composition and temperature position is located within a two-phase region, things are more complex. The tie line must be utilized in conjunction with a procedure that is often called the **lever rule** (or the *inverse lever rule*), which is applied as follows:

lever rule

1. The tie line is constructed across the two-phase region at the temperature of the alloy.
2. The overall alloy composition is located on the tie line.
3. The fraction of one phase is computed by taking the length of tie line from the overall alloy composition to the phase boundary for the *other* phase, and dividing by the total tie line length.

4. The fraction of the other phase is determined in the same manner.
5. If phase percentages are desired, each phase fraction is multiplied by 100. When the composition axis is scaled in weight percent, the phase fractions computed using the lever rule are mass fractions—the mass (or weight) of a specific phase divided by the total alloy mass (or weight). The mass of each phase is computed from the product of each phase fraction and the total alloy mass.

In the employment of the lever rule, tie line segment lengths may be determined either by direct measurement from the phase diagram using a linear scale, preferably graduated in millimeters, or by subtracting compositions as taken from the composition axis.

Consider again the example shown in Figure 9.3*b*, in which at 1250°C both α and liquid phases are present for a 35 wt% Ni–65 wt% Cu alloy. The problem is to compute the fraction of each of the α and liquid phases. The tie line has been constructed that was used for the determination of α and L phase compositions. Let the overall alloy composition be located along the tie line and denoted as C_0, and mass fractions be represented by W_L and W_α for the respective phases. From the lever rule, W_L may be computed according to

$$W_L = \frac{S}{R + S} \tag{9.1a}$$

or, by subtracting compositions,

Lever rule expression for computation of liquid mass fraction (per Figure 9.3*b*)

$$W_L = \frac{C_\alpha - C_0}{C_\alpha - C_L} \tag{9.1b}$$

Composition need be specified in terms of only one of the constituents for a binary alloy; for the preceding computation, weight percent nickel will be used (i.e., C_0 = 35 wt% Ni, C_α = 42.5 wt% Ni, and C_L = 31.5 wt% Ni), and

$$W_L = \frac{42.5 - 35}{42.5 - 31.5} = 0.68$$

Similarly, for the α phase,

Lever rule expression for computation of α-phase mass fraction (per Figure 9.3*b*)

$$W_\alpha = \frac{R}{R + S} \tag{9.2a}$$

$$= \frac{C_0 - C_L}{C_\alpha - C_L} \tag{9.2b}$$

$$= \frac{35 - 31.5}{42.5 - 31.5} = 0.32$$

Of course, identical answers are obtained if compositions are expressed in weight percent copper instead of nickel.

Thus, the lever rule may be employed to determine the relative amounts or fractions of phases in any two-phase region for a binary alloy if the temperature and composition are known and if equilibrium has been established. Its derivation is presented as an example problem.

It is easy to confuse the foregoing procedures for the determination of phase compositions and fractional phase amounts; thus, a brief summary is warranted. *Compositions* of phases are expressed in terms of weight percents of the components (e.g., wt% Cu, wt% Ni). For any alloy consisting of a single phase, the composition of that phase is the same as the total alloy composition. If two phases are present, the tie line must be employed, the extremities of which determine the compositions of the respective phases. With regard to *fractional phase amounts* (e.g., mass fraction of the α or liquid phase), when a single phase exists, the alloy is completely that phase. For a two-phase alloy, on the other hand, the lever rule is utilized, in which a ratio of tie line segment lengths is taken.

Concept Check 9.2

A copper–nickel alloy of composition 70 wt% Ni–30 wt% Cu is slowly heated from a temperature of 1300°C (2370°F).

(a) At what temperature does the first liquid phase form?

(b) What is the composition of this liquid phase?

(c) At what temperature does complete melting of the alloy occur?

(d) What is the composition of the last solid remaining prior to complete melting?

[*The answer may be found at www.wiley.com/college/callister (Student Companion Site).*]

Concept Check 9.3

Is it possible to have a copper–nickel alloy that, at equilibrium, consists of an α phase of composition 37 wt% Ni–63 wt% Cu, and also a liquid phase of composition 20 wt% Ni–80 wt% Cu? If so, what will be the approximate temperature of the alloy? If this is not possible, explain why.

[*The answer may be found at www.wiley.com/college/callister (Student Companion Site).*]

EXAMPLE PROBLEM 9.1

Lever Rule Derivation

Derive the lever rule.

Solution

Consider the phase diagram for copper and nickel (Figure 9.3*b*) and alloy of composition C_0 at 1250°C, and let C_α, C_L, W_α, and W_L represent the same parameters as given earlier. This derivation is accomplished through two conservation-of-mass expressions. With the first, because only two phases are present, the sum of their mass fractions must be equal to unity; that is,

$$W_\alpha + W_L = 1 \tag{9.3}$$

For the second, the mass of one of the components (either Cu or Ni) that is present in both of the phases must be equal to the mass of that component in the total alloy, or

$$W_\alpha C_\alpha + W_L C_L = C_0 \tag{9.4}$$

Simultaneous solution of these two equations leads to the lever rule expressions for this particular situation, Equations 9.1b and 9.2b:

$$W_L = \frac{C_\alpha - C_0}{C_\alpha - C_L} \tag{9.1b}$$

$$W_\alpha = \frac{C_0 - C_L}{C_\alpha - C_L} \tag{9.2b}$$

For multiphase alloys, it is often more convenient to specify relative phase amount in terms of volume fraction rather than mass fraction. Phase volume fractions are preferred because they (rather than mass fractions) may be determined from examination of the microstructure; furthermore, the properties of a multiphase alloy may be estimated on the basis of volume fractions.

For an alloy consisting of α and β phases, the volume fraction of the α phase, V_α, is defined as

α phase volume fraction—dependence on volumes of α and β phases

$$V_\alpha = \frac{v_\alpha}{v_\alpha + v_\beta} \tag{9.5}$$

where v_α and v_β denote the volumes of the respective phases in the alloy. Of course, an analogous expression exists for V_β, and, for an alloy consisting of just two phases, it is the case that $V_\alpha + V_\beta = 1$.

On occasion conversion from mass fraction to volume fraction (or vice versa) is desired. Equations that facilitate these conversions are as follows:

Conversion of mass fractions of α and β phases to volume fractions

$$V_\alpha = \frac{\dfrac{W_\alpha}{\rho_\alpha}}{\dfrac{W_\alpha}{\rho_\alpha} + \dfrac{W_\beta}{\rho_\beta}} \tag{9.6a}$$

$$V_\beta = \frac{\dfrac{W_\beta}{\rho_\beta}}{\dfrac{W_\alpha}{\rho_\alpha} + \dfrac{W_\beta}{\rho_\beta}} \tag{9.6b}$$

and

Conversion of volume fractions of α and β phases to mass fractions

$$W_\alpha = \frac{V_\alpha \rho_\alpha}{V_\alpha \rho_\alpha + V_\beta \rho_\beta} \tag{9.7a}$$

$$W_\beta = \frac{V_\beta \rho_\beta}{V_\alpha \rho_\alpha + V_\beta \rho_\beta} \tag{9.7b}$$

In these expressions, ρ_α and ρ_β are the densities of the respective phases; these may be determined approximately using Equations 4.10a and 4.10b.

When the densities of the phases in a two-phase alloy differ significantly, there will be quite a disparity between mass and volume fractions; conversely, if the phase densities are the same, mass and volume fractions are identical.

9.9 DEVELOPMENT OF MICROSTRUCTURE IN ISOMORPHOUS ALLOYS

Equilibrium Cooling

VMSE

Isomorphous (Sb-Bi)

At this point it is instructive to examine the development of microstructure that occurs for isomorphous alloys during solidification. We first treat the situation in which the cooling occurs very slowly, in that phase equilibrium is continuously maintained.

Let us consider the copper–nickel system (Figure 9.3*a*), specifically an alloy of composition 35 wt% Ni–65 wt% Cu as it is cooled from 1300°C. The region of the Cu–Ni phase diagram in the vicinity of this composition is shown in Figure 9.4. Cooling of an alloy of this composition corresponds to moving down the vertical dashed line. At 1300°C, point *a*, the alloy is completely liquid (of composition 35 wt% Ni–65 wt% Cu) and has the microstructure represented by the circle inset in the figure. As cooling begins, no microstructural or compositional changes will be realized until we reach the liquidus line (point *b*, ~1260°C). At this point,

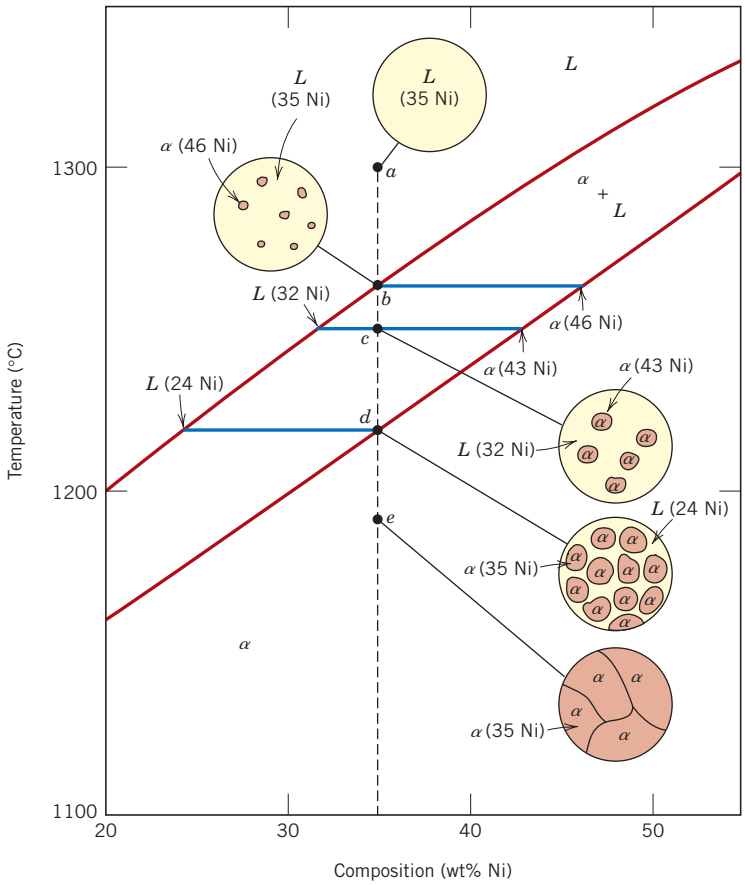

Figure 9.4 Schematic representation of the development of microstructure during the equilibrium solidification of a 35 wt% Ni–65 wt% Cu alloy.

the first solid α begins to form, which has a composition dictated by the tie line drawn at this temperature [i.e., 46 wt% Ni–54 wt% Cu, noted as α(46 Ni)]; the composition of liquid is still approximately 35 wt% Ni–65 wt% Cu [L(35 Ni)], which is different from that of the solid α. With continued cooling, both compositions and relative amounts of each of the phases will change. The compositions of the liquid and α phases will follow the liquidus and solidus lines, respectively. Furthermore, the fraction of the α phase will increase with continued cooling. Note that the overall alloy composition (35 wt% Ni–65 wt% Cu) remains unchanged during cooling even though there is a redistribution of copper and nickel between the phases.

At 1250°C, point c in Figure 9.4, the compositions of the liquid and α phases are 32 wt% Ni–68 wt% Cu [L(32 Ni)] and 43 wt% Ni–57 wt% Cu [α(43 Ni)], respectively.

The solidification process is virtually complete at about 1220°C, point d; the composition of the solid α is approximately 35 wt% Ni–65 wt% Cu (the overall alloy composition), whereas that of the last remaining liquid is 24 wt% Ni–76 wt% Cu. Upon crossing the solidus line, this remaining liquid solidifies; the final product then is a polycrystalline α-phase solid solution that has a uniform 35 wt% Ni–65 wt% Cu composition (point e, Figure 9.4). Subsequent cooling will produce no microstructural or compositional alterations.

Nonequilibrium Cooling

Conditions of equilibrium solidification and the development of microstructures, as described in the previous section, are realized only for extremely slow cooling rates. The reason for this is that with changes in temperature, there must be readjustments in the compositions of the liquid and solid phases in accordance with the phase diagram (i.e., with the liquidus and solidus lines), as discussed. These readjustments are accomplished by diffusional processes—that is, diffusion in both solid and liquid phases and also across the solid–liquid interface. Inasmuch as diffusion is a time-dependent phenomenon (Section 5.3), to maintain equilibrium during cooling, sufficient time must be allowed at each temperature for the appropriate compositional readjustments. Diffusion rates (i.e., the magnitudes of the diffusion coefficients) are especially low for the solid phase and, for both phases, decrease with diminishing temperature. In virtually all practical solidification situations, cooling rates are much too rapid to allow these compositional readjustments and maintenance of equilibrium; consequently, microstructures other than those previously described develop.

Some of the consequences of nonequilibrium solidification for isomorphous alloys will now be discussed by considering a 35 wt% Ni–65 wt% Cu alloy, the same composition that was used for equilibrium cooling in the previous section. The portion of the phase diagram near this composition is shown in Figure 9.5; in addition, microstructures and associated phase compositions at various temperatures upon cooling are noted in the circular insets. To simplify this discussion it will be assumed that diffusion rates in the liquid phase are sufficiently rapid such that equilibrium is maintained in the liquid.

Let us begin cooling from a temperature of about 1300°C; this is indicated by point a' in the liquid region. This liquid has a composition of 35 wt% Ni–65 wt% Cu [noted as L(35 Ni) in the figure], and no changes occur while cooling through the liquid phase region (moving down vertically from point a'). At point b' (approximately 1260°C), α-phase particles begin to form, which, from the tie line constructed, have a composition of 46 wt% Ni–54 wt% Cu [α(46 Ni)].

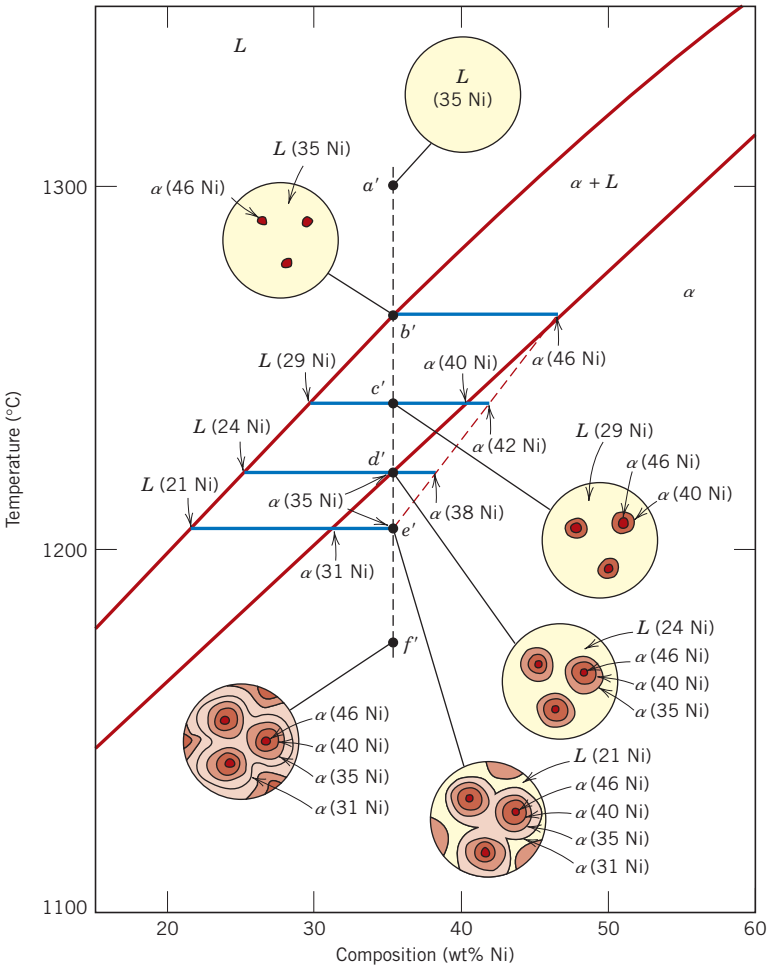

Figure 9.5 Schematic representation of the development of microstructure during the nonequilibrium solidification of a 35 wt% Ni–65 wt% Cu alloy.

Upon further cooling to point c' (about 1240°C), the liquid composition has shifted to 29 wt% Ni–71 wt% Cu; furthermore, at this temperature the composition of the α phase that solidified is 40 wt% Ni–60 wt% Cu [α(40 Ni)]. However, because diffusion in the solid α phase is relatively slow, the α phase that formed at point b' has not changed composition appreciably—that is, it is still about 46 wt% Ni—and the composition of the α grains has continuously changed with radial position, from 46 wt% Ni at grain centers to 40 wt% Ni at the outer grain perimeters. Thus, at point c', the *average composition* of the solid α grains that have formed would be some volume weighted average composition, lying between 46 and 40 wt% Ni. For the sake of argument, let us take this average composition to be 42 wt% Ni–58 wt% Cu [α(42 Ni)]. Furthermore, we would also find that, on the basis of lever-rule computations, a greater proportion of liquid is present for these nonequilibrium conditions than for equilibrium cooling. The implication of this nonequilibrium solidification phenomenon is that the solidus line on the phase diagram has been shifted to higher Ni contents—to the average compositions of the α phase (e.g., 42 wt% Ni at 1240°C)—and is represented by the dashed line in Figure 9.5. There is no comparable alteration of the liquidus line inasmuch as it is assumed that

equilibrium is maintained in the liquid phase during cooling because of sufficiently rapid diffusion rates.

At point d' (~1220°C) and for equilibrium cooling rates, solidification should be completed. However, for this nonequilibrium situation, there is still an appreciable proportion of liquid remaining, and the α phase that is forming has a composition of 35 wt% Ni [α(35 Ni)]; also the *average* α-phase composition at this point is 38 wt% Ni [α(38 Ni)].

Nonequilibrium solidification finally reaches completion at point e' (~1205°C). The composition of the last α phase to solidify at this point is about 31 wt% Ni; the *average* composition of the α phase at complete solidification is 35 wt% Ni. The inset at point f' shows the microstructure of the totally solid material.

The degree of displacement of the nonequilibrium solidus curve from the equilibrium one will depend on rate of cooling. The slower the cooling rate, the smaller this displacement; that is, the difference between the equilibrium solidus and average solid composition is lower. Furthermore, if the diffusion rate in the solid phase is increased, this displacement will be diminished.

There are some important consequences for isomorphous alloys that have solidified under nonequilibrium conditions. As discussed earlier, the distribution of the two elements within the grains is nonuniform, a phenomenon termed *segregation;* that is, concentration gradients are established across the grains that are represented by the insets of Figure 9.5. The center of each grain, which is the first part to freeze, is rich in the high-melting element (e.g., nickel for this Cu–Ni system), whereas the concentration of the low-melting element increases with position from this region to the grain boundary. This is termed a *cored* structure, which gives rise to less than the optimal properties. As a casting having a cored structure is reheated, grain boundary regions will melt first inasmuch as they are richer in the low-melting component. This produces a sudden loss in mechanical integrity due to the thin liquid film that separates the grains. Furthermore, this melting may begin at a temperature below the equilibrium solidus temperature of the alloy. Coring may be eliminated by a homogenization heat treatment carried out at a temperature below the solidus point for the particular alloy composition. During this process, atomic diffusion occurs, which produces compositionally homogeneous grains.

9.10 MECHANICAL PROPERTIES OF ISOMORPHOUS ALLOYS

We shall now briefly explore how the mechanical properties of solid isomorphous alloys are affected by composition as other structural variables (e.g., grain size) are held constant. For all temperatures and compositions below the melting temperature of the lowest-melting component, only a single solid phase will exist. Therefore, each component will experience solid-solution strengthening (Section 7.9), or an increase in strength and hardness by additions of the other component. This effect is demonstrated in Figure 9.6*a* as tensile strength versus composition for the copper–nickel system at room temperature; at some intermediate composition, the curve necessarily passes through a maximum. Plotted in Figure 9.6*b* is the ductility (%EL)–composition behavior, which is just the opposite of tensile strength; that is, ductility decreases with additions of the second component, and the curve exhibits a minimum.

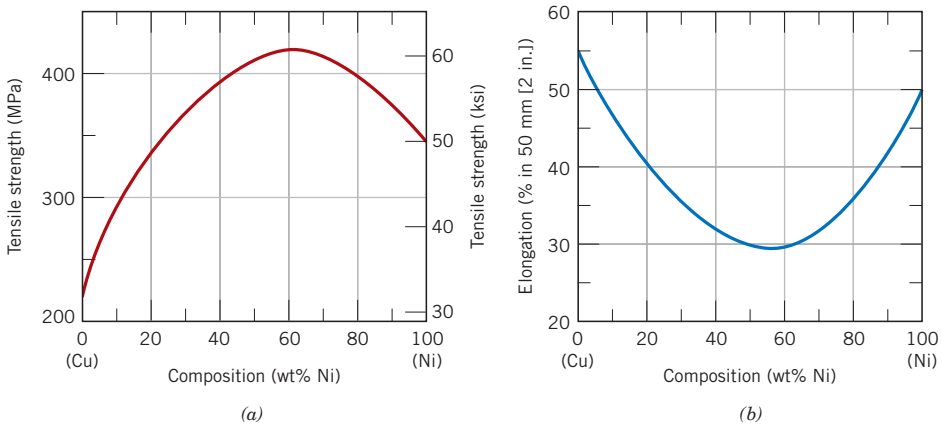

Figure 9.6 For the copper–nickel system, (*a*) tensile strength versus composition, and (*b*) ductility (%EL) versus composition at room temperature. A solid solution exists over all compositions for this system.

9.11 BINARY EUTECTIC SYSTEMS

Another type of common and relatively simple phase diagram found for binary alloys is shown in Figure 9.7 for the copper–silver system; this is known as a binary eutectic phase diagram. A number of features of this phase diagram are important and worth noting. First, three single-phase regions are found on the diagram: α, β, and liquid. The α phase is a solid solution rich in copper; it has silver as the solute

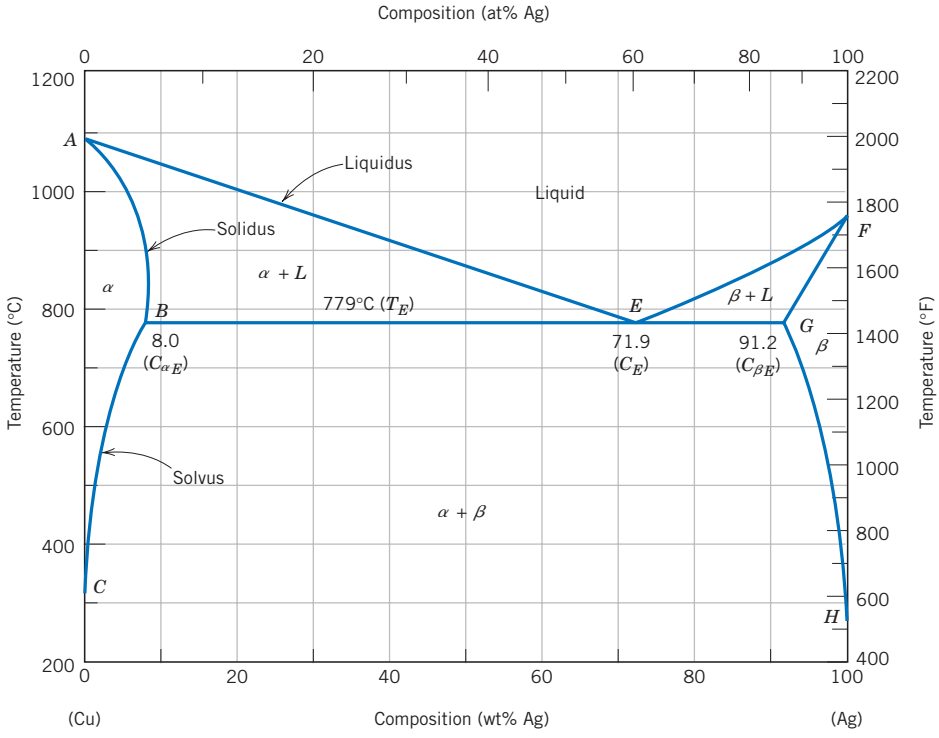

Figure 9.7 The copper–silver phase diagram. [Adapted from *Binary Alloy Phase Diagrams,* 2nd edition, Vol. 1, T. B. Massalski (Editor-in-Chief), 1990. Reprinted by permission of ASM International, Materials Park, OH.]

component and an FCC crystal structure. The β-phase solid solution also has an FCC structure, but copper is the solute. Pure copper and pure silver are also considered to be α and β phases, respectively.

Thus, the solubility in each of these solid phases is limited, in that at any temperature below line BEG only a limited concentration of silver will dissolve in copper (for the α phase), and similarly for copper in silver (for the β phase). The solubility limit for the α phase corresponds to the boundary line, labeled CBA, between the $\alpha/(\alpha + \beta)$ and $\alpha/(\alpha + L)$ phase regions; it increases with temperature to a maximum [8.0 wt% Ag at 779°C (1434°F)] at point B, and decreases back to zero at the melting temperature of pure copper, point A [1085°C (1985°F)]. At temperatures below 779°C (1434°F), the solid solubility limit line separating the α and $\alpha + \beta$ phase regions is termed a **solvus line;** the boundary AB between the α and $\alpha + L$ fields is the **solidus line,** as indicated in Figure 9.7. For the β phase, both solvus and solidus lines also exist, HG and GF, respectively, as shown. The maximum solubility of copper in the β phase, point G (8.8 wt% Cu), also occurs at 779°C (1434°F). This horizontal line BEG, which is parallel to the composition axis and extends between these maximum solubility positions, may also be considered a solidus line; it represents the lowest temperature at which a liquid phase may exist for any copper–silver alloy that is at equilibrium.

solvus line

solidus line

There are also three two-phase regions found for the copper–silver system (Figure 9.7): $\alpha + L$, $\beta + L$, and $\alpha + \beta$. The α- and β-phase solid solutions coexist for all compositions and temperatures within the $\alpha + \beta$ phase field; the α + liquid and β + liquid phases also coexist in their respective phase regions. Furthermore, compositions and relative amounts for the phases may be determined using tie lines and the lever rule as outlined previously.

As silver is added to copper, the temperature at which the alloys become totally liquid decreases along the **liquidus line,** line AE; thus, the melting temperature of copper is lowered by silver additions. The same may be said for silver: the introduction of copper reduces the temperature of complete melting along the other liquidus line, FE. These liquidus lines meet at the point E on the phase diagram, through which also passes the horizontal isotherm line BEG. Point E is called an **invariant point,** which is designated by the composition C_E and temperature T_E; for the copper–silver system, the values of C_E and T_E are 71.9 wt% Ag and 779°C (1434°F), respectively.

liquidus line

invariant point

An important reaction occurs for an alloy of composition C_E as it changes temperature in passing through T_E; this reaction may be written as follows:

The eutectic reaction (per Figure 9.7)

$$L(C_E) \underset{\text{heating}}{\overset{\text{cooling}}{\rightleftharpoons}} \alpha(C_{\alpha E}) + \beta(C_{\beta E}) \tag{9.8}$$

Or, upon cooling, a liquid phase is transformed into the two solid α and β phases at the temperature T_E; the opposite reaction occurs upon heating. This is called a **eutectic reaction** (*eutectic* means "easily melted"), and C_E and T_E represent the eutectic composition and temperature, respectively; $C_{\alpha E}$ and $C_{\beta E}$ are the respective compositions of the α and β phases at T_E. Thus, for the copper–silver system, the eutectic reaction, Equation 9.8, may be written as follows:

eutectic reaction

$$L(71.9\text{ wt\% Ag}) \underset{\text{heating}}{\overset{\text{cooling}}{\rightleftharpoons}} \alpha(8.0\text{ wt\% Ag}) + \beta(91.2\text{ wt\% Ag})$$

Often, the horizontal solidus line at T_E is called the *eutectic isotherm*.

The eutectic reaction, upon cooling, is similar to solidification for pure components in that the reaction proceeds to completion at a constant temperature, or isothermally, at T_E. However, the solid product of eutectic solidification is always two solid phases, whereas for a pure component only a single phase forms. Because of this eutectic reaction, phase diagrams similar to that in Figure 9.7 are termed *eutectic phase diagrams*; components exhibiting this behavior comprise a *eutectic system*.

In the construction of binary phase diagrams, it is important to understand that one or at most two phases may be in equilibrium within a phase field. This holds true for the phase diagrams in Figures 9.3*a* and 9.7. For a eutectic system, three phases (α, β, and L) may be in equilibrium, but only at points along the eutectic isotherm. Another general rule is that single-phase regions are always separated from each other by a two-phase region that consists of the two single phases that it separates. For example, the $\alpha + \beta$ field is situated between the α and β single-phase regions in Figure 9.7.

Another common eutectic system is that for lead and tin; the phase diagram (Figure 9.8) has a general shape similar to that for copper–silver. For the lead–tin system the solid-solution phases are also designated by α and β; in this case, α represents a solid solution of tin in lead and, for β, tin is the solvent and lead is the solute. The eutectic invariant point is located at 61.9 wt% Sn and 183°C (361°F). Of course, maximum solid solubility compositions as well as component melting temperatures will be different for the copper–silver and lead–tin systems, as may be observed by comparing their phase diagrams.

On occasion, low-melting-temperature alloys are prepared having near-eutectic compositions. A familiar example is the 60–40 solder, containing 60 wt% Sn and

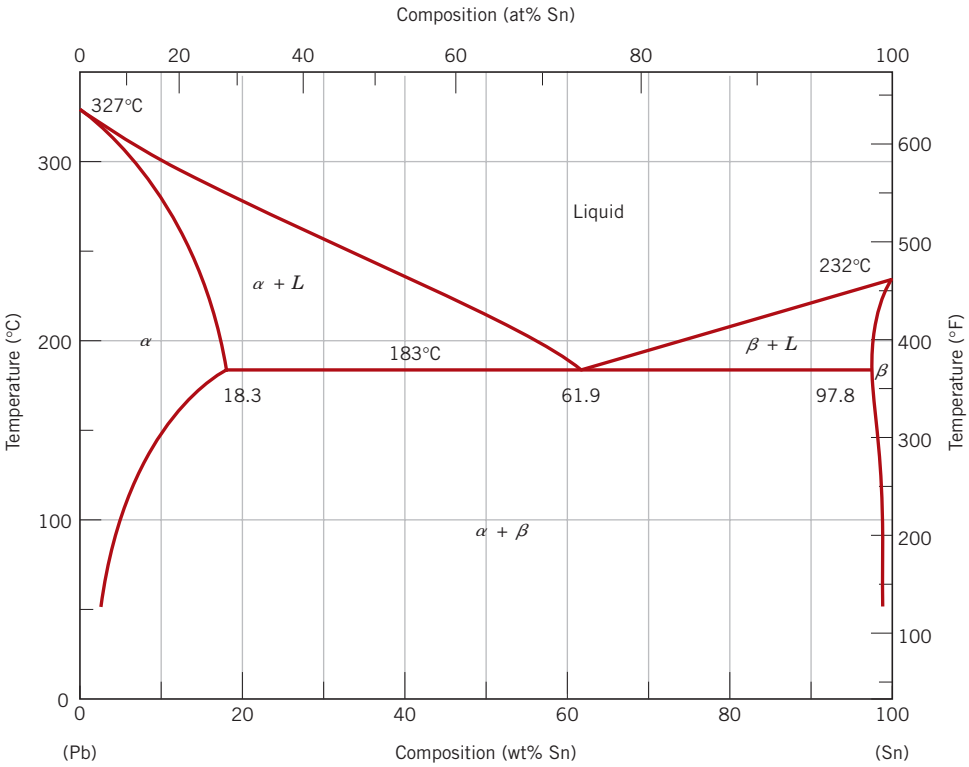

Figure 9.8 The lead–tin phase diagram. [Adapted from *Binary Alloy Phase Diagrams,* 2nd edition, Vol. 3, T. B. Massalski (Editor-in-Chief), 1990. Reprinted by permission of ASM International, Materials Park, OH.]

40 wt% Pb. Figure 9.8 indicates that an alloy of this composition is completely molten at about 185°C (365°F), which makes this material especially attractive as a low-temperature solder, because it is easily melted.

Concept Check 9.4

At 700°C (1290°F), what is the maximum solubility **(a)** of Cu in Ag? **(b)** Of Ag in Cu?

[*The answer may be found at www.wiley.com/college/callister (Student Companion Site).*]

Concept Check 9.5

The following is a portion of the H_2O–NaCl phase diagram:

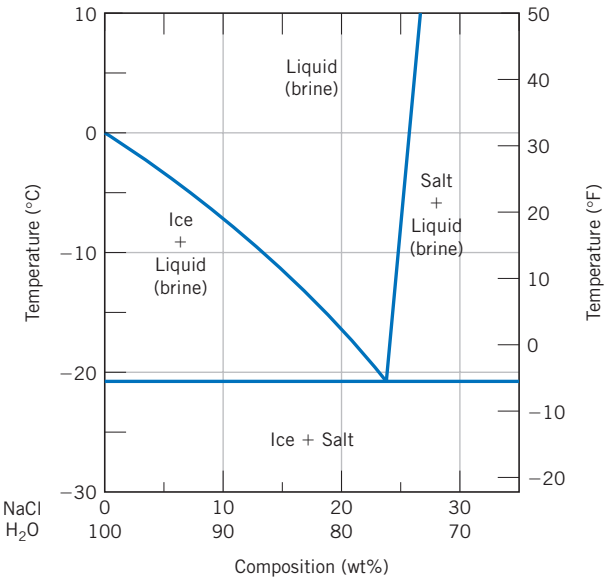

(a) Using this diagram, briefly explain how spreading salt on ice that is at a temperature below 0°C (32°F) can cause the ice to melt.

(b) At what temperature is salt no longer useful in causing ice to melt?

[*The answer may be found at www.wiley.com/college/callister (Student Companion Site).*]

EXAMPLE PROBLEM 9.2

Determination of Phases Present and Computation of Phase Compositions

For a 40 wt% Sn–60 wt% Pb alloy at 150°C (300°F), **(a)** what phase(s) is (are) present? **(b)** What is (are) the composition(s) of the phase(s)?

Solution

(a) Locate this temperature–composition point on the phase diagram (point *B* in Figure 9.9). Inasmuch as it is within the $\alpha + \beta$ region, both α and β phases will coexist.

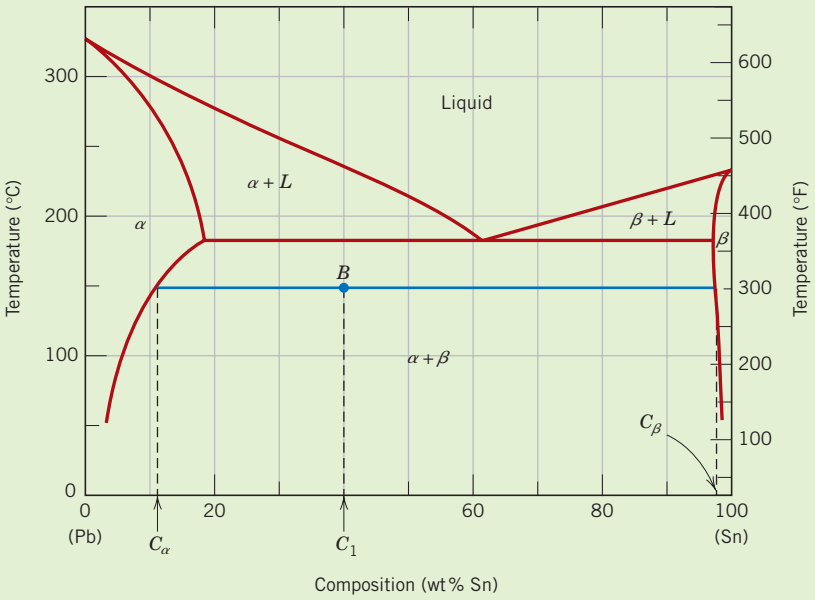

Figure 9.9 The lead–tin phase diagram. For a 40 wt% Sn–60 wt% Pb alloy at 150°C (point B), phase compositions and relative amounts are computed in Example Problems 9.2 and 9.3.

(b) Because two phases are present, it becomes necessary to construct a tie line across the $\alpha + \beta$ phase field at 150°C, as indicated in Figure 9.9. The composition of the α phase corresponds to the tie line intersection with the $\alpha/(\alpha + \beta)$ solvus phase boundary—about 11 wt% Sn–89 wt% Pb, denoted as C_α. Similarly for the β phase, which will have a composition of approximately 98 wt% Sn–2 wt% Pb (C_β).

EXAMPLE PROBLEM 9.3

Relative Phase Amount Determinations—Mass and Volume Fractions

For the lead–tin alloy in Example Problem 9.2, calculate the relative amount of each phase present in terms of **(a)** mass fraction and **(b)** volume fraction. At 150°C take the densities of Pb and Sn to be 11.23 and 7.24 g/cm^3, respectively.

Solution

(a) Because the alloy consists of two phases, it is necessary to employ the lever rule. If C_1 denotes the overall alloy composition, mass fractions may be computed by subtracting compositions, in terms of weight percent tin, as follows:

$$W_\alpha = \frac{C_\beta - C_1}{C_\beta - C_\alpha} = \frac{98 - 40}{98 - 11} = 0.67$$

$$W_\beta = \frac{C_1 - C_\alpha}{C_\beta - C_\alpha} = \frac{40 - 11}{98 - 11} = 0.33$$

(b) To compute volume fractions it is first necessary to determine the density of each phase using Equation 4.10a. Thus

$$\rho_\alpha = \frac{100}{\dfrac{C_{\mathrm{Sn}(\alpha)}}{\rho_{\mathrm{Sn}}} + \dfrac{C_{\mathrm{Pb}(\alpha)}}{\rho_{\mathrm{Pb}}}}$$

where $C_{\mathrm{Sn}(\alpha)}$ and $C_{\mathrm{Pb}(\alpha)}$ denote the concentrations in weight percent of tin and lead, respectively, in the α phase. From Example Problem 9.2, these values are 11 wt% and 89 wt%. Incorporation of these values along with the densities of the two components leads to

$$\rho_\alpha = \frac{100}{\dfrac{11}{7.24\ \mathrm{g/cm^3}} + \dfrac{89}{11.23\ \mathrm{g/cm^3}}} = 10.59\ \mathrm{g/cm^3}$$

Similarly for the β phase:

$$\rho_\beta = \frac{100}{\dfrac{C_{\mathrm{Sn}(\beta)}}{\rho_{\mathrm{Sn}}} + \dfrac{C_{\mathrm{Pb}(\beta)}}{\rho_{\mathrm{Pb}}}}$$

$$= \frac{100}{\dfrac{98}{7.24\ \mathrm{g/cm^3}} + \dfrac{2}{11.23\ \mathrm{g/cm^3}}} = 7.29\ \mathrm{g/cm^3}$$

Now it becomes necessary to employ Equations 9.6a and 9.6b to determine V_α and V_β as

$$V_\alpha = \frac{\dfrac{W_\alpha}{\rho_\alpha}}{\dfrac{W_\alpha}{\rho_\alpha} + \dfrac{W_\beta}{\rho_\beta}}$$

$$= \frac{\dfrac{0.67}{10.59\ \mathrm{g/cm^3}}}{\dfrac{0.67}{10.59\ \mathrm{g/cm^3}} + \dfrac{0.33}{7.29\ \mathrm{g/cm^3}}} = 0.58$$

$$V_\beta = \frac{\dfrac{W_\beta}{\rho_\beta}}{\dfrac{W_\alpha}{\rho_\alpha} + \dfrac{W_\beta}{\rho_\beta}}$$

$$= \frac{\dfrac{0.33}{7.29\ \mathrm{g/cm^3}}}{\dfrac{0.67}{10.59\ \mathrm{g/cm^3}} + \dfrac{0.33}{7.29\ \mathrm{g/cm^3}}} = 0.42$$

MATERIALS OF IMPORTANCE

Lead-Free Solders

Solders are metal alloys that are used to bond or join two or more components (usually other metal alloys). They are used extensively in the electronics industry to physically hold assemblies together; furthermore, they must allow expansion and contraction of the various components, must transmit electrical signals, and also dissipate any heat that is generated. The bonding action is accomplished by melting the solder material, allowing it to flow among and make contact with the components to be joined (which do not melt), and, finally, upon solidification, forming a physical bond with all of these components.

In the past, the vast majority of solders have been lead–tin alloys. These materials are reliable and inexpensive and have relatively low melting temperatures. The most common lead–tin solder has a composition of 63 wt% Sn–37 wt% Pb. According to the lead–tin phase diagram, Figure 9.8, this composition is near the eutectic and has a melting temperature of about 183°C, the lowest temperature possible with the existence of a liquid phase (at equilibrium) for the lead–tin system. It follows that this alloy is often called a "eutectic lead–tin solder."

Unfortunately, lead is a mildly toxic metal, and there is serious concern about the environmental impact of discarded lead-containing products that can leach into groundwater from landfills or pollute the air if incinerated. Consequently, in some countries legislation has been enacted that bans the use of lead-containing solders. This has forced the development of lead-free solders that, among other things, must have relatively low melting temperatures (or temperature ranges). Some of these are ternary alloys (i.e., composed of three metals), to include tin–silver–copper and tin–silver–bismuth solders. The compositions of several lead-free solders are listed in Table 9.1.

Of course, melting temperatures (or temperature ranges) are important in the development and selection of these new solder alloys, information that is available from phase diagrams. For example, the tin–bismuth phase diagram is presented in Figure 9.10. Here it may be noted that a eutectic exists at 57 wt% Bi and 139°C, which are indeed the composition and melting temperature of the Bi–Sn solder in Table 9.1.

Table 9.1 Compositions, Solidus Temperatures, and Liquidus Temperatures for Five Lead-Free Solders

Composition (wt%)	*Solidus Temperature (°C)*	*Liquidus Temperature (°C)*
52 In/48 Sn*	118	118
57 Bi/43 Sn*	139	139
91.8 Sn/3.4 Ag/4.8 Bi	211	213
95.5 Sn/3.8 Ag/0.7 Cu*	217	217
99.3 Sn/0.7 Cu*	227	227

*The compositions of these alloys are eutectic compositions; therefore, their solidus and liquidus temperatures are identical.

Source: Adapted from E. Bastow, "Solder Families and How They Work," *Advanced Materials & Processes,* Vol. 161, No. 12, M. W. Hunt (Editor-in-chief), ASM International, 2003, p. 28. Reprinted by permission of ASM International, Materials Park, OH.

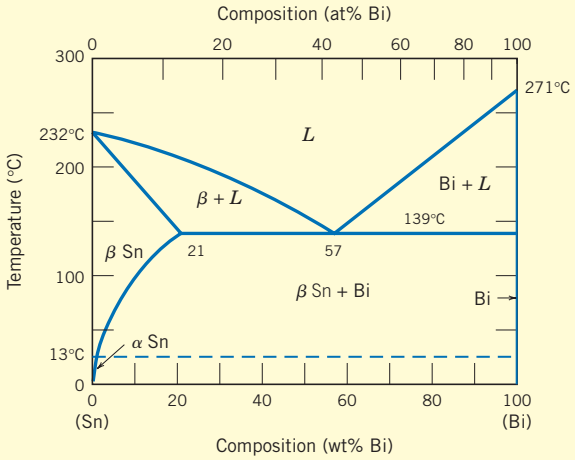

Figure 9.10 The tin–bismuth phase diagram. [Adapted from *ASM Handbook,* Vol. 3, *Alloy Phase Diagrams,* H. Baker (Editor), ASM International, 1992, p. 2.106. Reprinted by permission of ASM International, Materials Park, OH.]

9.12 DEVELOPMENT OF MICROSTRUCTURE IN EUTECTIC ALLOYS

Depending on composition, several different types of microstructures are possible for the slow cooling of alloys belonging to binary eutectic systems. These possibilities will be considered in terms of the lead–tin phase diagram, Figure 9.8.

The first case is for compositions ranging between a pure component and the maximum solid solubility for that component at room temperature [20°C (70°F)]. For the lead–tin system, this includes lead-rich alloys containing between 0 and about 2 wt% Sn (for the α-phase solid solution), and also between approximately 99 wt% Sn and pure tin (for the β phase). For example, consider an alloy of composition C_1 (Figure 9.11) as it is slowly cooled from a temperature within the liquid-phase region, say, 350°C; this corresponds to moving down the dashed vertical line ww' in the figure. The alloy remains totally liquid and of composition C_1 until we cross the liquidus line at approximately 330°C, at which time the solid α phase begins to form. While passing through this narrow $\alpha + L$ phase region, solidification proceeds in the same manner as was described for the copper–nickel alloy in the preceding section; that is, with continued cooling more of the solid α forms. Furthermore, liquid- and solid-phase compositions are different, which follow along the liquidus and solidus phase boundaries, respectively. Solidification reaches completion at the point where ww' crosses the solidus line. The resulting alloy is polycrystalline with a uniform composition of C_1, and no subsequent changes will occur

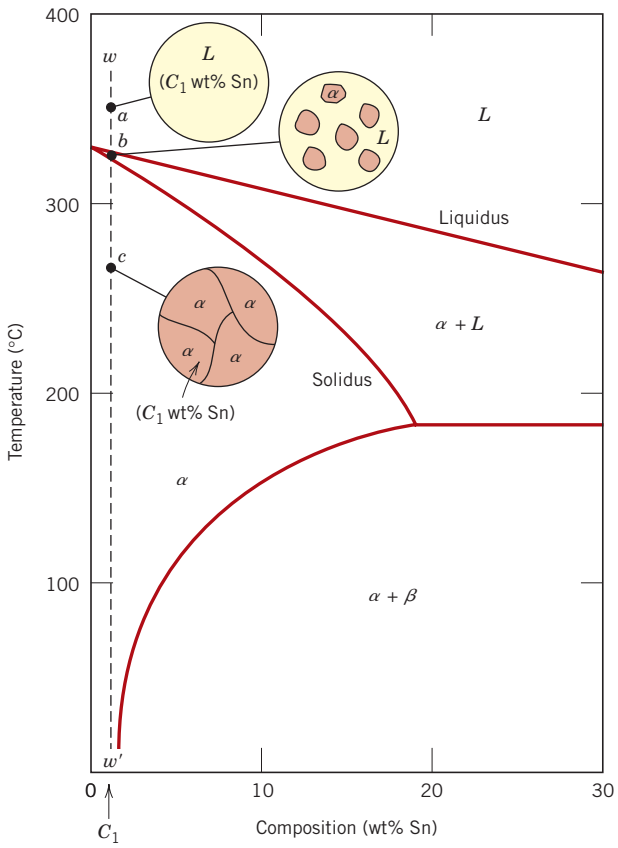

Figure 9.11 Schematic representations of the equilibrium microstructures for a lead–tin alloy of composition C_1 as it is cooled from the liquid-phase region.

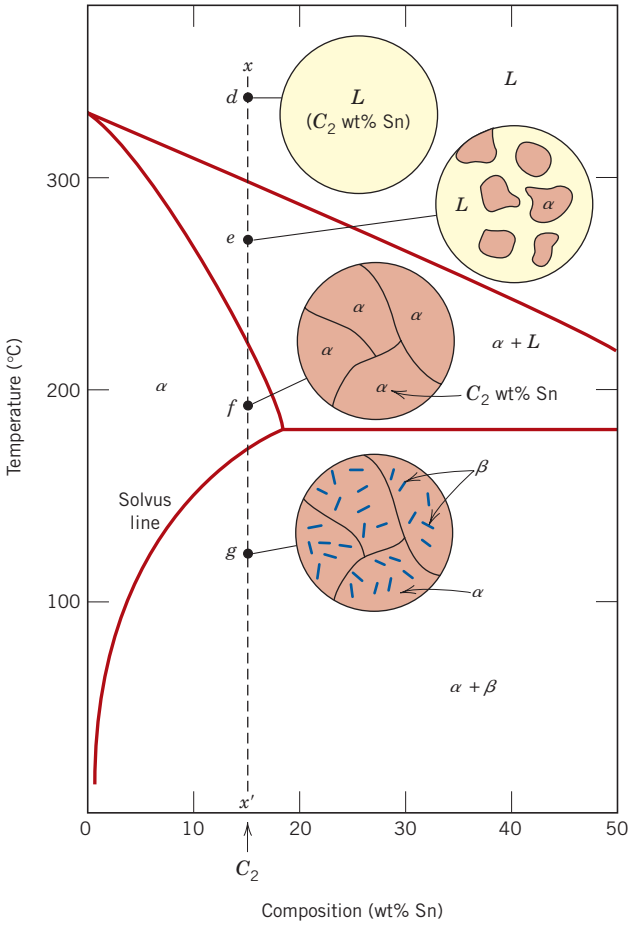

Figure 9.12 Schematic representations of the equilibrium microstructures for a lead–tin alloy of composition C_2 as it is cooled from the liquid-phase region.

upon cooling to room temperature. This microstructure is represented schematically by the inset at point *c* in Figure 9.11.

The second case considered is for compositions that range between the room temperature solubility limit and the maximum solid solubility at the eutectic temperature. For the lead–tin system (Figure 9.8), these compositions extend from about 2 wt% Sn to 18.3 wt% Sn (for lead-rich alloys) and from 97.8 wt% Sn to approximately 99 wt% Sn (for tin-rich alloys). Let us examine an alloy of composition C_2 as it is cooled along the vertical line xx' in Figure 9.12. Down to the intersection of xx' and the solvus line, changes that occur are similar to the previous case, as we pass through the corresponding phase regions (as demonstrated by the insets at points *d*, *e*, and *f*). Just above the solvus intersection, point *f*, the microstructure consists of α grains of composition C_2. Upon crossing the solvus line, the α solid solubility is exceeded, which results in the formation of small β-phase particles; these are indicated in the microstructure inset at point *g*. With continued cooling, these particles will grow in size because the mass fraction of the β phase increases slightly with decreasing temperature.

Eutectic (Pb-Sn)

The third case involves solidification of the eutectic composition, 61.9 wt% Sn (C_3 in Figure 9.13). Consider an alloy having this composition that is cooled from a temperature within the liquid-phase region (e.g., 250°C) down the vertical line yy' in Figure 9.13. As the temperature is lowered, no changes occur until we reach the eutectic

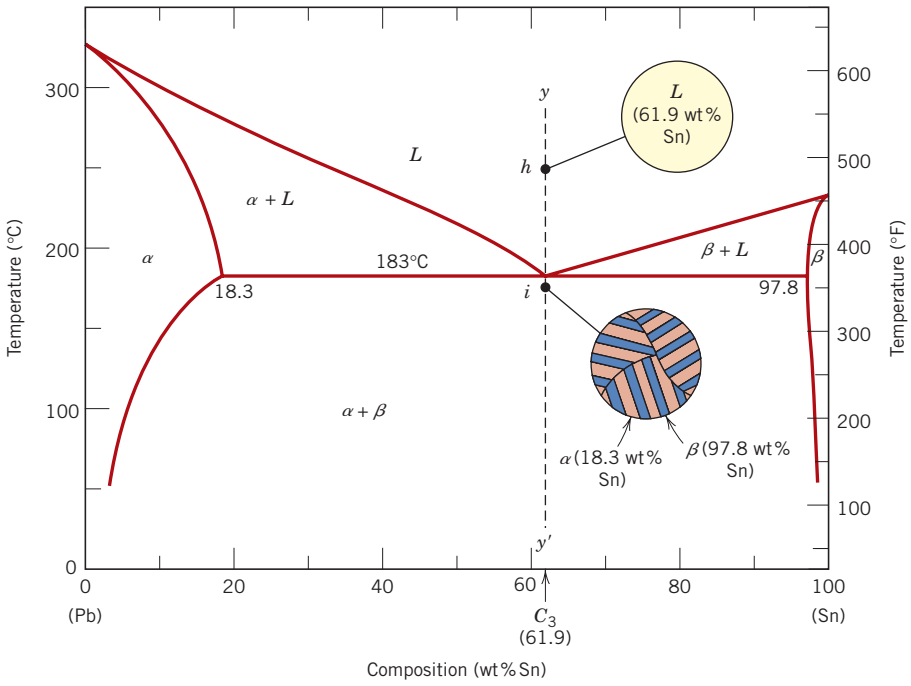

Figure 9.13 Schematic representations of the equilibrium microstructures for a lead–tin alloy of eutectic composition C_3 above and below the eutectic temperature.

temperature, 183°C. Upon crossing the eutectic isotherm, the liquid transforms to the two α and β phases. This transformation may be represented by the reaction

$$L(61.9\text{ wt\% Sn}) \underset{\text{heating}}{\overset{\text{cooling}}{\rightleftharpoons}} \alpha(18.3\text{ wt\% Sn}) + \beta(97.8\text{ wt\% Sn}) \tag{9.9}$$

in which the α- and β-phase compositions are dictated by the eutectic isotherm end points.

During this transformation, there must necessarily be a redistribution of the lead and tin components, inasmuch as the α and β phases have different compositions neither of which is the same as that of the liquid (as indicated in Equation 9.9). This redistribution is accomplished by atomic diffusion. The microstructure of the solid that results from this transformation consists of alternating layers (sometimes called lamellae) of the α and β phases that form simultaneously during the transformation. This microstructure, represented schematically in Figure 9.13, point i, is called a **eutectic structure** and is characteristic of this reaction. A photomicrograph of this structure for the lead–tin eutectic is shown in Figure 9.14. Subsequent cooling of the

eutectic structure

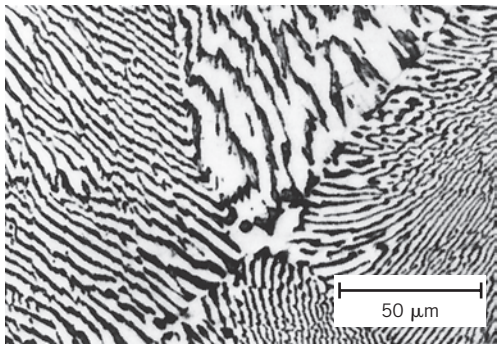

Figure 9.14 Photomicrograph showing the microstructure of a lead–tin alloy of eutectic composition. This microstructure consists of alternating layers of a lead-rich α-phase solid solution (dark layers), and a tin-rich β-phase solid solution (light layers). 375 ×. (Reproduced with permission from *Metals Handbook,* 9th edition, Vol. 9, *Metallography and Microstructures,* American Society for Metals, Materials Park, OH, 1985.)

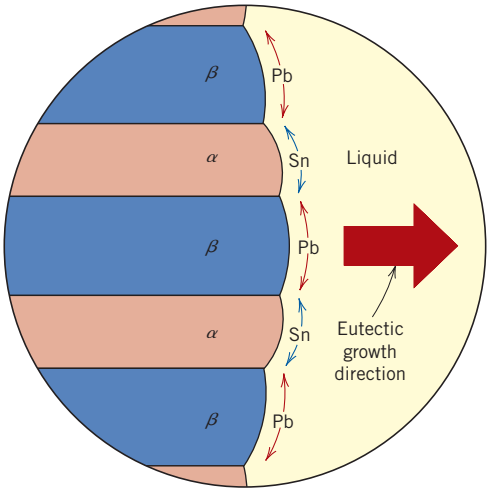

Figure 9.15 Schematic representation of the formation of the eutectic structure for the lead–tin system. Directions of diffusion of tin and lead atoms are indicated by blue and red arrows, respectively.

alloy from just below the eutectic to room temperature will result in only minor microstructural alterations.

The microstructural change that accompanies this eutectic transformation is represented schematically in Figure 9.15; here is shown the α–β layered eutectic growing into and replacing the liquid phase. The process of the redistribution of lead and tin occurs by diffusion in the liquid just ahead of the eutectic–liquid interface. The arrows indicate the directions of diffusion of lead and tin atoms; lead atoms diffuse toward the α-phase layers because this α phase is lead-rich (18.3 wt% Sn–81.7 wt% Pb); conversely, the direction of diffusion of tin is in the direction of the β, tin-rich (97.8 wt% Sn–2.2 wt% Pb) layers. The eutectic structure forms in these alternating layers because, for this lamellar configuration, atomic diffusion of lead and tin need only occur over relatively short distances.

The fourth and final microstructural case for this system includes all compositions other than the eutectic that, when cooled, cross the eutectic isotherm. Consider, for example, the composition C_4, Figure 9.16, which lies to the left of the eutectic; as the temperature is lowered, we move down the line zz', beginning at point j. The microstructural development between points j and l is similar to that for the second case, such that just prior to crossing the eutectic isotherm (point l), the α and liquid phases are present having compositions of approximately 18.3 and 61.9 wt% Sn, respectively, as determined from the appropriate tie line. As the temperature is lowered to just below the eutectic, the liquid phase, which is of the eutectic composition, will transform to the eutectic structure (i.e., alternating α and β lamellae); insignificant changes will occur with the α phase that formed during cooling through the $\alpha + L$ region. This microstructure is represented schematically by the inset at point m in Figure 9.16. Thus, the α phase will be present both in the eutectic structure and also as the phase that formed while cooling through the $\alpha + L$ phase field. To distinguish one α from the other, that which resides in the eutectic structure is called **eutectic** α, while the other that formed prior to crossing the eutectic isotherm is termed **primary** α; both are labeled in Figure 9.16. The photomicrograph in Figure 9.17 is of a lead–tin alloy in which both primary α and eutectic structures are shown.

eutectic phase

primary phase

In dealing with microstructures, it is sometimes convenient to use the term **microconstituent**—that is, an element of the microstructure having an identifiable

microconstituent

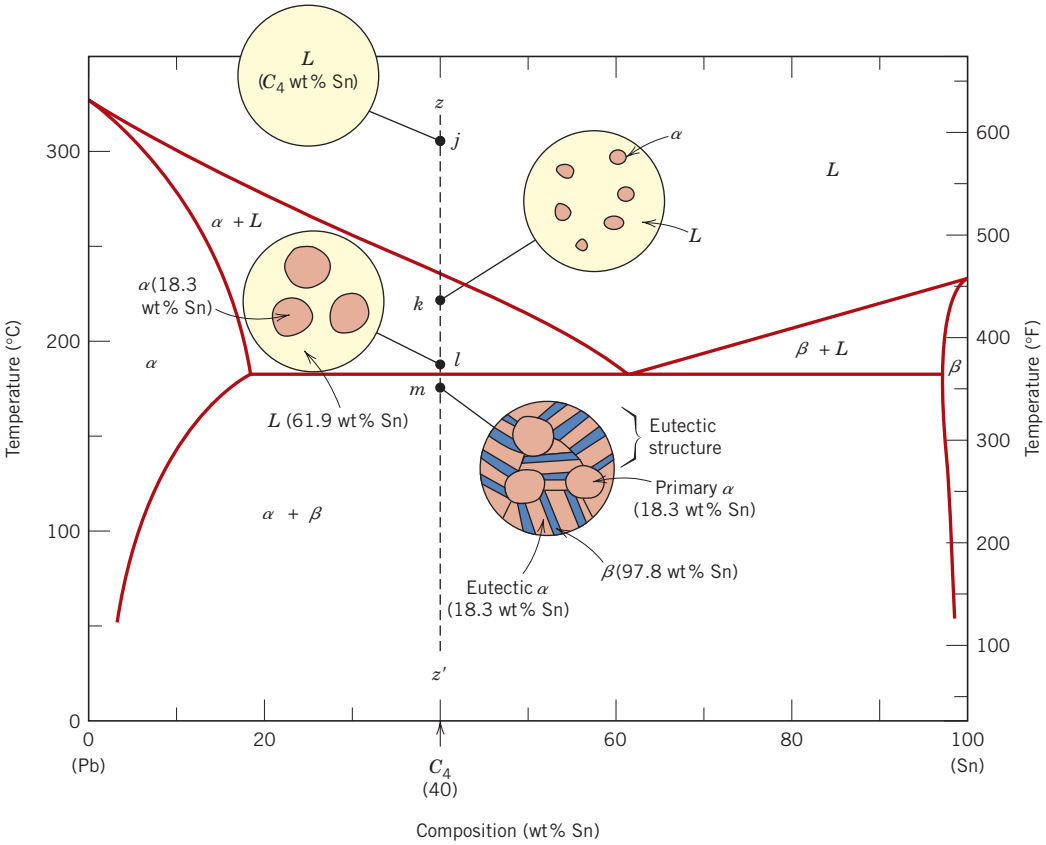

Figure 9.16 Schematic representations of the equilibrium microstructures for a lead–tin alloy of composition C_4 as it is cooled from the liquid-phase region.

and characteristic structure. For example, in the point *m* inset, Figure 9.16, there are two microconstituents—namely, primary α and the eutectic structure. Thus, the eutectic structure is a microconstituent even though it is a mixture of two phases, because it has a distinct lamellar structure, with a fixed ratio of the two phases.

It is possible to compute the relative amounts of both eutectic and primary α microconstituents. Because the eutectic microconstituent always forms from the

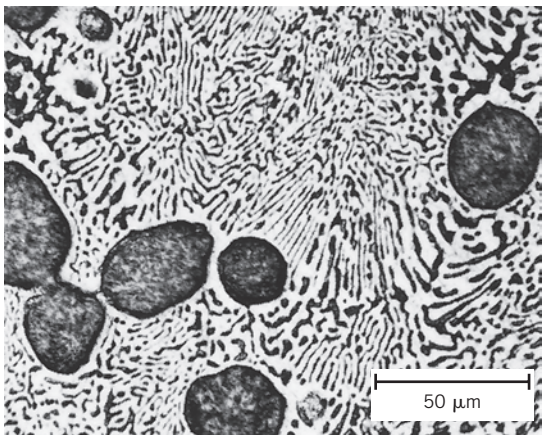

Figure 9.17 Photomicrograph showing the microstructure of a lead–tin alloy of composition 50 wt% Sn–50 wt% Pb. This microstructure is composed of a primary lead-rich α phase (large dark regions) within a lamellar eutectic structure consisting of a tin-rich β phase (light layers) and a lead-rich α phase (dark layers). 400×. (Reproduced with permission from *Metals Handbook,* 9th edition, Vol. 9, *Metallography and Microstructures,* American Society for Metals, Materials Park, OH, 1985.)

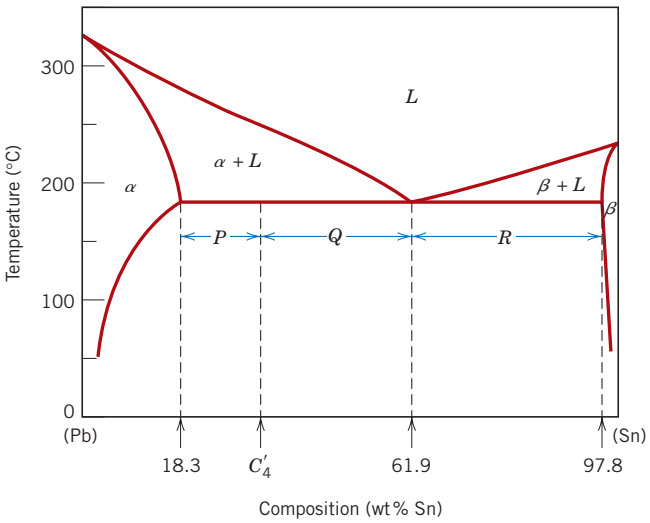

Figure 9.18 The lead–tin phase diagram used in computations for relative amounts of primary α and eutectic microconstituents for an alloy of composition C_4'.

liquid having the eutectic composition, this microconstituent may be assumed to have a composition of 61.9 wt% Sn. Hence, the lever rule is applied using a tie line between the α–$(\alpha + \beta)$ phase boundary (18.3 wt% Sn) and the eutectic composition. For example, consider the alloy of composition C_4' in Figure 9.18. The fraction of the eutectic microconstituent W_e is just the same as the fraction of liquid W_L from which it transforms, or

Lever rule expression for computation of eutectic microconstituent and liquid phase mass fractions (composition C_4', Figure 9.18)

$$W_e = W_L = \frac{P}{P + Q}$$

$$= \frac{C_4' - 18.3}{61.9 - 18.3} = \frac{C_4' - 18.3}{43.6} \tag{9.10}$$

Furthermore, the fraction of primary α, $W_{\alpha'}$, is just the fraction of the α phase that existed prior to the eutectic transformation or, from Figure 9.18,

Lever rule expression for computation of primary α-phase mass fraction

$$W_{\alpha'} = \frac{Q}{P + Q}$$

$$= \frac{61.9 - C_4'}{61.9 - 18.3} = \frac{61.9 - C_4'}{43.6} \tag{9.11}$$

The fractions of *total* α, W_α (both eutectic and primary), and also of total β, W_β, are determined by use of the lever rule and a tie line that extends *entirely across the* $\alpha + \beta$ *phase field*. Again, for an alloy having composition C_4',

Lever rule expression for computation of total α-phase mass fraction

$$W_\alpha = \frac{Q + R}{P + Q + R}$$

$$= \frac{97.8 - C_4'}{97.8 - 18.3} = \frac{97.8 - C_4'}{79.5} \tag{9.12}$$

and

Lever rule expression for computation of total β-phase mass fraction

$$W_\beta = \frac{P}{P + Q + R}$$

$$= \frac{C'_4 - 18.3}{97.8 - 18.3} = \frac{C'_4 - 18.3}{79.5} \tag{9.13}$$

Analogous transformations and microstructures result for alloys having compositions to the right of the eutectic (i.e., between 61.9 and 97.8 wt% Sn). However, below the eutectic temperature, the microstructure will consist of the eutectic and primary β microconstituents because, upon cooling from the liquid, we pass through the β + liquid phase field.

When, for case 4 (represented in Figure 9.16), conditions of equilibrium are not maintained while passing through the α (or β) + liquid phase region, the following consequences will be realized for the microstructure upon crossing the eutectic isotherm: (1) grains of the primary microconstituent will be cored, that is, have a nonuniform distribution of solute across the grains; and (2) the fraction of the eutectic microconstituent formed will be greater than for the equilibrium situation.

9.13 EQUILIBRIUM DIAGRAMS HAVING INTERMEDIATE PHASES OR COMPOUNDS

The isomorphous and eutectic phase diagrams discussed thus far are relatively simple, but those for many binary alloy systems are much more complex. The eutectic copper–silver and lead–tin phase diagrams (Figures 9.7 and 9.8) have only two solid phases, α and β; these are sometimes termed **terminal solid solutions,** because they exist over composition ranges near the concentration extremities of the phase diagram. For other alloy systems, **intermediate solid solutions** (or *intermediate phases*) may be found at other than the two composition extremes. Such is the case for the copper–zinc system. Its phase diagram (Figure 9.19) may at first appear formidable because there are some invariant points and reactions similar to the eutectic that have not yet been discussed. In addition, there are six different solid solutions—two terminal (α and η) and four intermediate (β, γ, δ, and ϵ). (The β', phase is termed an ordered solid solution, one in which the copper and zinc atoms are situated in a specific and ordered arrangement within each unit cell.) Some phase boundary lines near the bottom of Figure 9.19 are dashed to indicate that their positions have not been exactly determined. The reason for this is that at low temperatures, diffusion rates are very slow and inordinately long times are required to attain equilibrium. Again, only single- and two-phase regions are found on the diagram, and the same rules outlined in Section 9.8 are used to compute phase compositions and relative amounts. The commercial brasses are copper-rich copper–zinc alloys; for example, cartridge brass has a composition of 70 wt% Cu–30 wt% Zn and a microstructure consisting of a single α phase.

terminal solid solution

intermediate solid solution

For some systems, discrete intermediate compounds rather than solid solutions may be found on the phase diagram, and these compounds have distinct chemical formulas; for metal–metal systems, they are called **intermetallic compounds.** For example, consider the magnesium–lead system (Figure 9.20). The compound Mg_2Pb

intermetallic compound

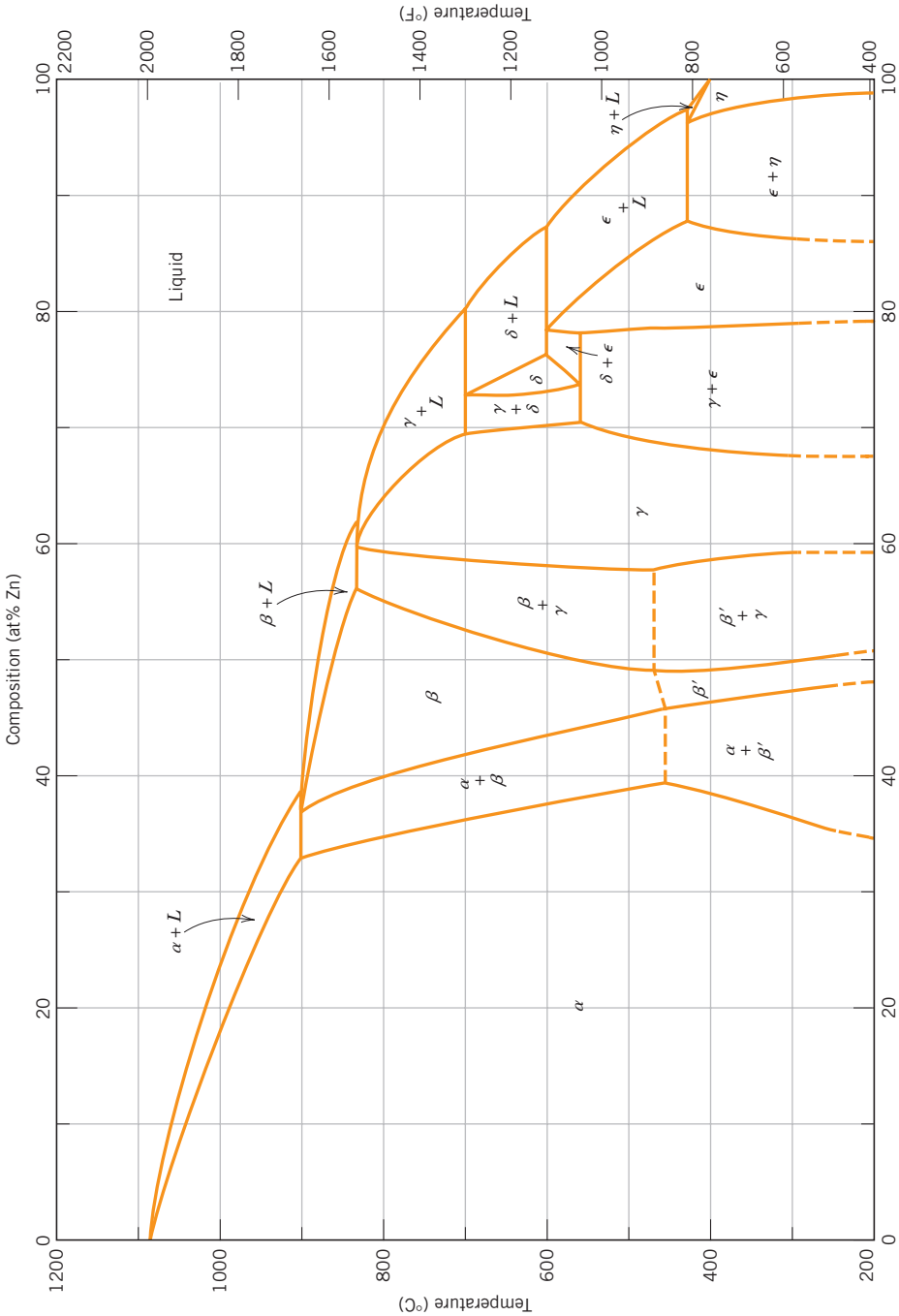

Figure 9.19 The copper–zinc phase diagram. [Adapted from *Binary Alloy Phase Diagrams*, 2nd edition, Vol. 2, T. B. Massalski (Editor-in-Chief), 1990. Reprinted by permission of ASM International, Materials Park, OH.]

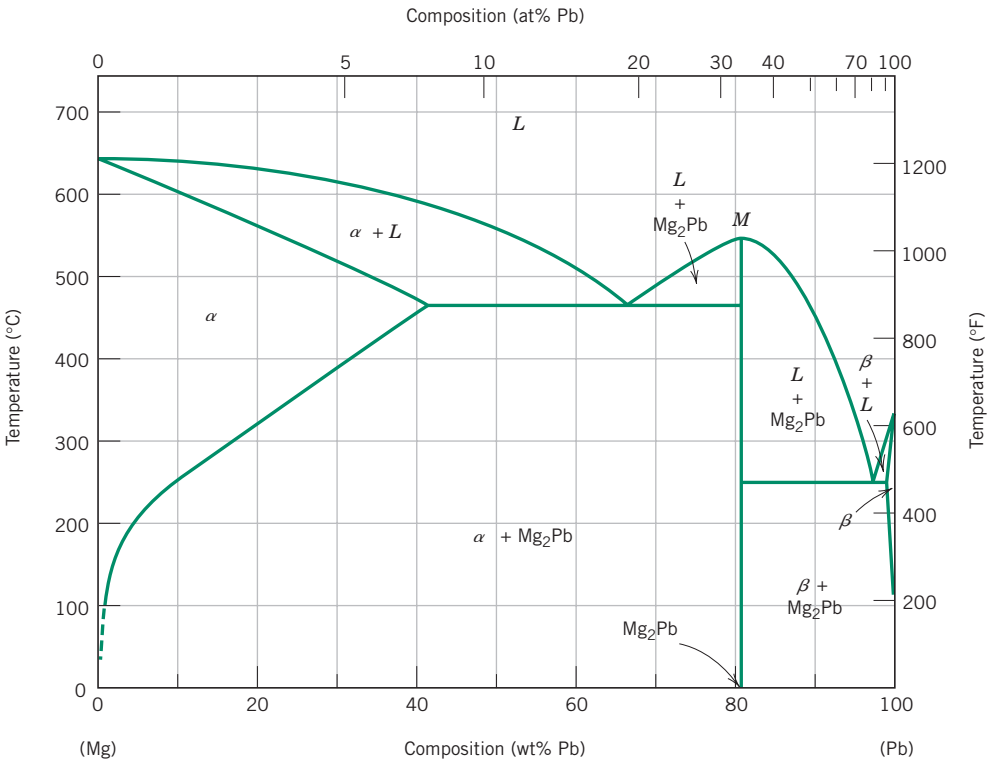

Figure 9.20 The magnesium–lead phase diagram. [Adapted from *Phase Diagrams of Binary Magnesium Alloys,* A. A. Nayeb-Hashemi and J. B. Clark (Editors), 1988. Reprinted by permission of ASM International, Materials Park, OH.]

has a composition of 19 wt% Mg–81 wt% Pb (33 at% Pb), and is represented as a vertical line on the diagram, rather than as a phase region of finite width; hence, Mg_2Pb can exist by itself only at this precise composition.

Several other characteristics are worth noting for this magnesium–lead system. First, the compound Mg_2Pb melts at approximately 550°C (1020°F), as indicated by point *M* in Figure 9.20. Also, the solubility of lead in magnesium is rather extensive, as indicated by the relatively large composition span for the α-phase field. On the other hand, the solubility of magnesium in lead is extremely limited. This is evident from the very narrow β terminal solid-solution region on the right or lead-rich side of the diagram. Finally, this phase diagram may be thought of as two simple eutectic diagrams joined back to back, one for the Mg–Mg_2Pb system and the other for Mg_2Pb–Pb; as such, the compound Mg_2Pb is really considered to be a component. This separation of complex phase diagrams into smaller-component units may simplify them and, furthermore, expedite their interpretation.

9.14 EUTECTOID AND PERITECTIC REACTIONS

In addition to the eutectic, other invariant points involving three different phases are found for some alloy systems. One of these occurs for the copper–zinc system (Figure 9.19) at 560°C (1040°F) and 74 wt% Zn–26 wt% Cu. A portion of

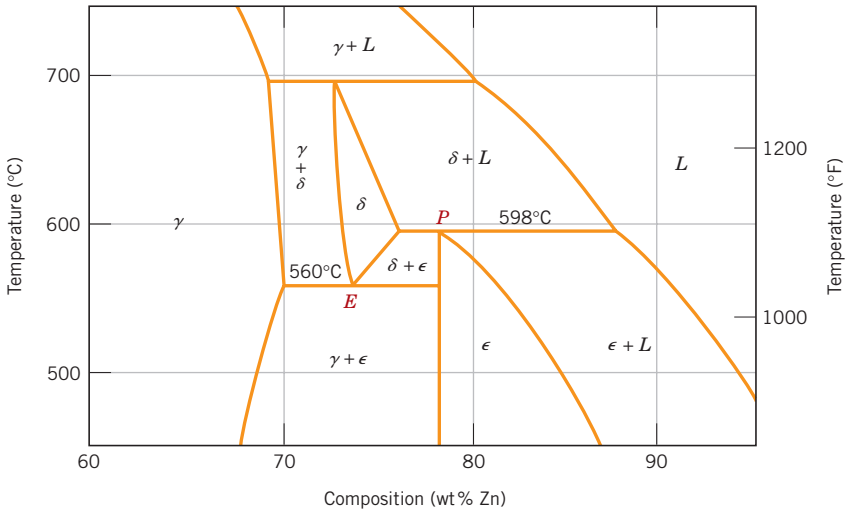

Figure 9.21 A region of the copper–zinc phase diagram that has been enlarged to show eutectoid and peritectic invariant points, labeled *E* (560°C, 74 wt% Zn) and *P* (598°C, 78.6 wt% Zn), respectively. [Adapted from *Binary Alloy Phase Diagrams,* 2nd edition, Vol. 2, T. B. Massalski (Editor-in-Chief), 1990. Reprinted by permission of ASM International, Materials Park, OH.]

the phase diagram in this vicinity appears enlarged in Figure 9.21. Upon cooling, a solid δ phase transforms into two other solid phases (γ and ϵ) according to the reaction

The eutectoid reaction (per point *E*, Figure 9.21)

$$\delta \underset{\text{heating}}{\overset{\text{cooling}}{\rightleftharpoons}} \gamma + \epsilon \tag{9.14}$$

eutectoid reaction

The reverse reaction occurs upon heating. It is called a **eutectoid** (or eutectic-like) **reaction,** and the invariant point (point *E*, Figure 9.21) and the horizontal tie line at 560°C are termed the *eutectoid* and *eutectoid isotherm,* respectively. The feature distinguishing "eutectoid" from "eutectic" is that one solid phase instead of a liquid transforms into two other solid phases at a single temperature. A eutectoid reaction is found in the iron–carbon system (Section 9.18) that is very important in the heat treating of steels.

peritectic reaction

The **peritectic reaction** is yet another invariant reaction involving three phases at equilibrium. With this reaction, upon heating, one solid phase transforms into a liquid phase and another solid phase. A peritectic exists for the copper–zinc system (Figure 9.21, point *P*) at 598°C (1108°F) and 78.6 wt% Zn–21.4 wt% Cu; this reaction is as follows:

The peritectic reaction (per point *P,* Figure 9.21)

$$\delta + L \underset{\text{heating}}{\overset{\text{cooling}}{\rightleftharpoons}} \epsilon \tag{9.15}$$

The low-temperature solid phase may be an intermediate solid solution (e.g., ϵ in the preceding reaction), or it may be a terminal solid solution. One of the latter peritectics exists at about 97 wt% Zn and 435°C (815°F) (see Figure 9.19), wherein the η phase, when heated, transforms to ϵ and liquid phases. Three other peritectics are found for the Cu–Zn system, the reactions of which involve β, δ, and γ intermediate solid solutions as the low-temperature phases that transform upon heating.

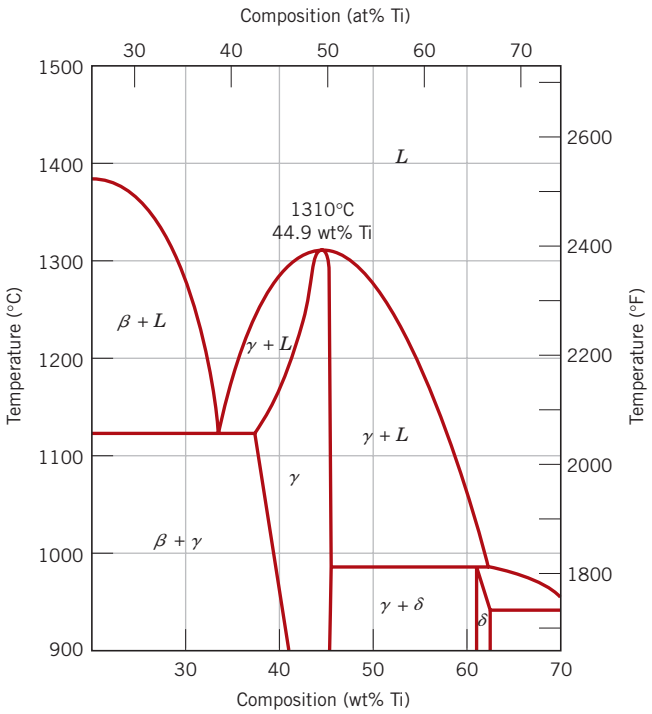

Figure 9.22 A portion of the nickel–titanium phase diagram on which is shown a congruent melting point for the γ-phase solid solution at 1310°C and 44.9 wt% Ti. [Adapted from *Phase Diagrams of Binary Nickel Alloys*, P. Nash (Editor), 1991. Reprinted by permission of ASM International, Materials Park, OH.]

9.15 CONGRUENT PHASE TRANSFORMATIONS

congruent transformation

Phase transformations may be classified according to whether there is any change in composition for the phases involved. Those for which there are no compositional alterations are said to be **congruent transformations.** Conversely, for *incongruent transformations,* at least one of the phases will experience a change in composition. Examples of congruent transformations include allotropic transformations (Section 3.6) and melting of pure materials. Eutectic and eutectoid reactions, as well as the melting of an alloy that belongs to an isomorphous system, all represent incongruent transformations.

Intermediate phases are sometimes classified on the basis of whether they melt congruently or incongruently. The intermetallic compound Mg_2Pb melts congruently at the point designated *M* on the magnesium–lead phase diagram, Figure 9.20. Also, for the nickel–titanium system, Figure 9.22, there is a congruent melting point for the γ solid solution that corresponds to the point of tangency for the pairs of liquidus and solidus lines, at 1310°C and 44.9 wt% Ti. Furthermore, the peritectic reaction is an example of incongruent melting for an intermediate phase.

Concept Check 9.6

The following figure is the hafnium–vanadium phase diagram, for which only single-phase regions are labeled. Specify temperature–composition points at which all eutectics, eutectoids, peritectics, and congruent phase transformations occur. Also, for each, write the reaction upon cooling. [Phase diagram from *ASM Handbook,* Vol. 3, *Alloy Phase Diagrams,* H. Baker (Editor), 1992, p. 2.244. Reprinted by permission of ASM International, Materials Park, OH.]

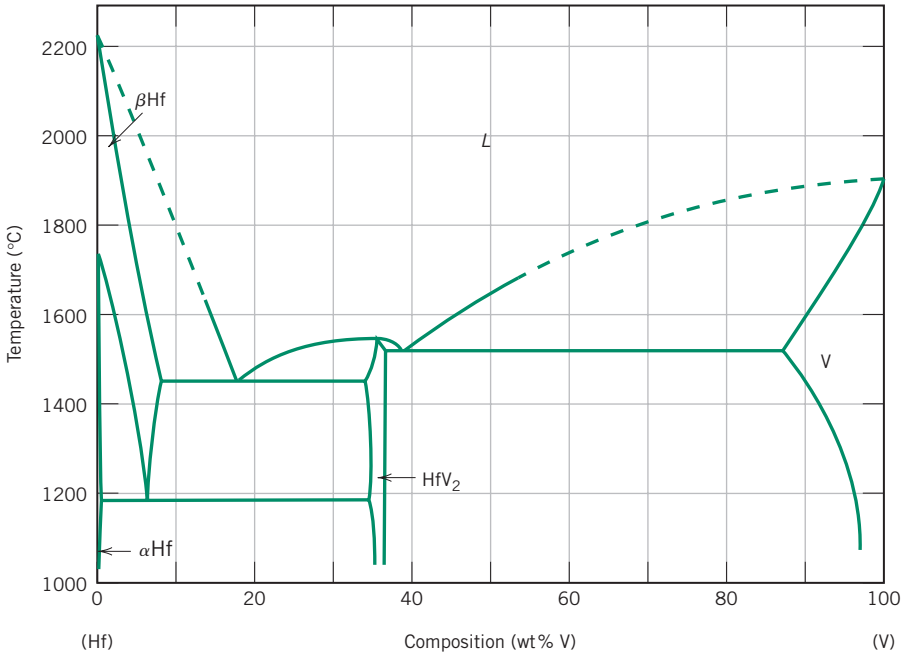

[*The answer may be found at www.wiley.com/college/callister (Student Companion Site).*]

9.16 CERAMIC AND TERNARY PHASE DIAGRAMS

It need not be assumed that phase diagrams exist only for metal–metal systems; in fact, phase diagrams that are very useful in the design and processing of ceramic systems have been experimentally determined for quite a number of these materials. Ceramic phase diagrams are discussed in Section 12.7.

Phase diagrams have also been determined for metallic (as well as ceramic) systems containing more than two components; however, their representation and interpretation may be exceedingly complex. For example, a ternary, or three-component, composition–temperature phase diagram in its entirety is depicted by a three-dimensional model. Portrayal of features of the diagram or model in two dimensions is possible but somewhat difficult.

9.17 THE GIBBS PHASE RULE

Gibbs phase rule

The construction of phase diagrams as well as some of the principles governing the conditions for phase equilibria are dictated by laws of thermodynamics. One of these is the **Gibbs phase rule,** proposed by the nineteenth-century physicist J. Willard Gibbs. This rule represents a criterion for the number of phases that will coexist within a system at equilibrium, and is expressed by the simple equation

General form of the Gibbs phase rule

$$P + F = C + N \tag{9.16}$$

where P is the number of phases present (the phase concept is discussed in Section 9.3). The parameter F is termed the *number of degrees of freedom* or the number of externally controlled variables (e.g., temperature, pressure, composition) which must be specified to completely define the state of the system. Expressed another way,

F is the number of these variables that can be changed independently without altering the number of phases that coexist at equilibrium. The parameter C in Equation 9.16 represents the number of components in the system. Components are normally elements or stable compounds and, in the case of phase diagrams, are the materials at the two extremities of the horizontal compositional axis (e.g., H_2O and $C_{12}H_{22}O_{11}$, and Cu and Ni for the phase diagrams shown in Figures 9.1 and 9.3*a*, respectively). Finally, N in Equation 9.16 is the number of noncompositional variables (e.g., temperature and pressure).

Let us demonstrate the phase rule by applying it to binary temperature–composition phase diagrams, specifically the copper–silver system, Figure 9.7. Because pressure is constant (1 atm), the parameter N is 1—temperature is the only noncompositional variable. Equation 9.16 now takes the form

$$P + F = C + 1 \tag{9.17}$$

Furthermore, the number of components C is 2 (Cu and Ag), and

$$P + F = 2 + 1 = 3$$

or

$$F = 3 - P$$

Consider the case of single-phase fields on the phase diagram (e.g., α, β, and liquid regions). Because only one phase is present, $P = 1$ and

$$\begin{aligned} F &= 3 - P \\ &= 3 - 1 = 2 \end{aligned}$$

This means that to completely describe the characteristics of any alloy that exists within one of these phase fields, we must specify two parameters; these are composition and temperature, which locate, respectively, the horizontal and vertical positions of the alloy on the phase diagram.

For the situation wherein two phases coexist, for example, $\alpha + L$, $\beta + L$, and $\alpha + \beta$ phase regions, Figure 9.7, the phase rule stipulates that we have but one degree of freedom because

$$\begin{aligned} F &= 3 - P \\ &= 3 - 2 = 1 \end{aligned}$$

Thus, it is necessary to specify either temperature or the composition of one of the phases to completely define the system. For example, suppose that we decide to specify temperature for the $\alpha + L$ phase region, say, T_1 in Figure 9.23. The compositions of the α and liquid phases (C_α and C_L) are thus dictated by the extremities of the tie line constructed at T_1 across the $\alpha + L$ field. Note that only the nature of the phases is important in this treatment and not the relative phase amounts. This is to say that the overall alloy composition could lie anywhere along this tie line constructed at temperature T_1 and still give C_α and C_L compositions for the respective α and liquid phases.

The second alternative is to stipulate the composition of one of the phases for this two-phase situation, which thereby fixes completely the state of the system. For example, if we specified C_α as the composition of the α phase that is in equilibrium with the liquid (Figure 9.23), then both the temperature of the alloy (T_1) and the composition of the liquid phase (C_L) are established, again by the tie line drawn across the $\alpha + L$ phase field so as to give this C_α composition.

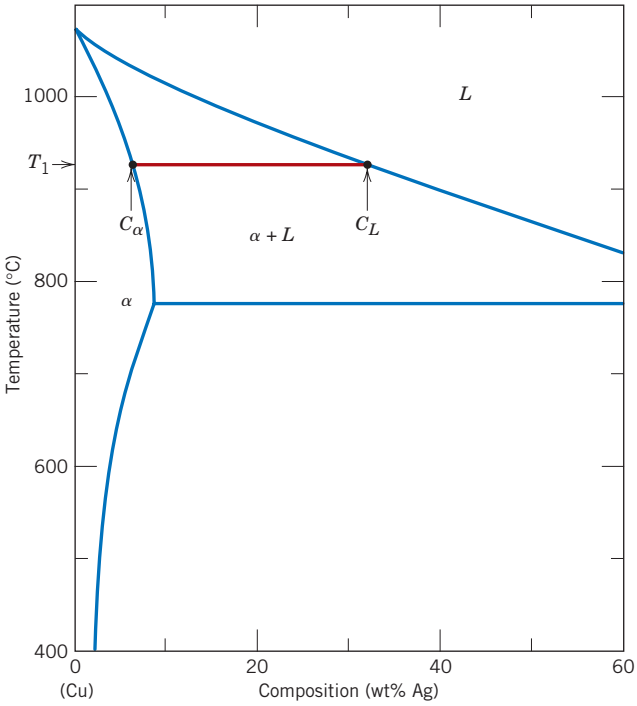

Figure 9.23 Enlarged copper-rich section of the Cu–Ag phase diagram in which the Gibbs phase rule for the coexistence of two phases (α and L) is demonstrated. Once the composition of either phase (C_α or C_L) or the temperature (T_1) is specified, values for the two remaining parameters are established by construction of the appropriate tie line.

For binary systems, when three phases are present, there are no degrees of freedom, because

$$F = 3 - P$$
$$= 3 - 3 = 0$$

This means that the compositions of all three phases as well as the temperature are fixed. This condition is met for a eutectic system by the eutectic isotherm; for the Cu–Ag system (Figure 9.7), it is the horizontal line that extends between points B and G. At this temperature, 779°C, the points at which each of the α, L, and β phase fields touch the isotherm line correspond to the respective phase compositions; namely, the composition of the α phase is fixed at 8.0 wt% Ag, that of the liquid at 71.9 wt% Ag, and that of the β phase at 91.2 wt% Ag. Thus, three-phase equilibrium will not be represented by a phase field, but rather by the unique horizontal isotherm line. Furthermore, all three phases will be in equilibrium for any alloy composition that lies along the length of the eutectic isotherm (e.g., for the Cu–Ag system at 779°C and compositions between 8.0 and 91.2 wt% Ag).

One use of the Gibbs phase rule is in analyzing for nonequilibrium conditions. For example, a microstructure for a binary alloy that developed over a range of temperatures and consisting of three phases is a nonequilibrium one; under these circumstances, three phases will exist only at a single temperature.

Concept Check 9.7

For a ternary system, three components are present; temperature is also a variable. What is the maximum number of phases that may be present for a ternary system, assuming that pressure is held constant?

[*The answer may be found at www.wiley.com/college/callister (Student Companion Site).*]

The Iron–Carbon System

Of all binary alloy systems, the one that is possibly the most important is that for iron and carbon. Both steels and cast irons, primary structural materials in every technologically advanced culture, are essentially iron–carbon alloys. This section is devoted to a study of the phase diagram for this system and the development of several of the possible microstructures. The relationships among heat treatment, microstructure, and mechanical properties are explored in Chapters 10 and 11.

9.18 THE IRON–IRON CARBIDE ($Fe–Fe_3C$) PHASE DIAGRAM

ferrite

austenite

A portion of the iron–carbon phase diagram is presented in Figure 9.24. Pure iron, upon heating, experiences two changes in crystal structure before it melts. At room temperature the stable form, called **ferrite,** or α-iron, has a BCC crystal structure. Ferrite experiences a polymorphic transformation to FCC **austenite,** or γ-iron, at 912°C (1674°F). This austenite persists to 1394°C (2541°F), at which temperature the FCC austenite reverts back to a BCC phase known as δ-ferrite, which finally

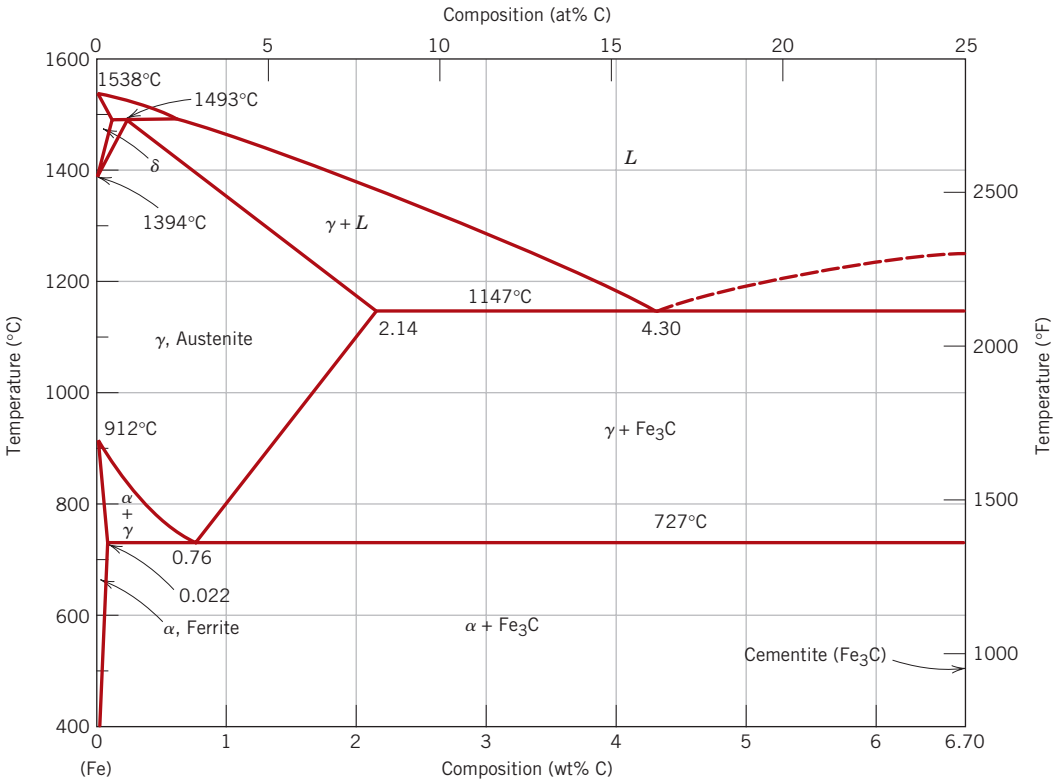

Figure 9.24 The iron–iron carbide phase diagram. [Adapted from *Binary Alloy Phase Diagrams,* 2nd edition, Vol. 1, T. B. Massalski (Editor-in-Chief), 1990. Reprinted by permission of ASM International, Materials Park, OH.]

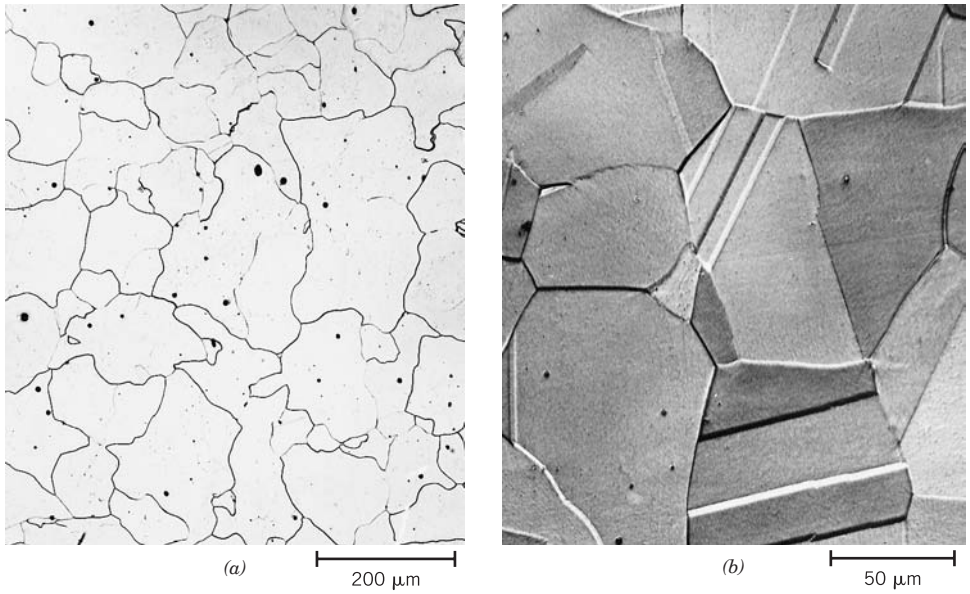

Figure 9.25 Photomicrographs of (*a*) α-ferrite (90×) and (*b*) austenite (325×). (Copyright 1971 by United States Steel Corporation.)

melts at 1538°C (2800°F). All these changes are apparent along the left vertical axis of the phase diagram.[1]

cementite

The composition axis in Figure 9.24 extends only to 6.70 wt% C; at this concentration the intermediate compound iron carbide, or **cementite** (Fe_3C), is formed, which is represented by a vertical line on the phase diagram. Thus, the iron–carbon system may be divided into two parts: an iron-rich portion, as in Figure 9.24, and the other (not shown) for compositions between 6.70 and 100 wt% C (pure graphite). In practice, all steels and cast irons have carbon contents less than 6.70 wt% C; therefore, we consider only the iron–iron carbide system. Figure 9.24 would be more appropriately labeled the Fe–Fe_3C phase diagram, because Fe_3C is now considered to be a component. Convention and convenience dictate that composition still be expressed in "wt% C" rather than "wt% Fe_3C"; 6.70 wt% C corresponds to 100 wt% Fe_3C.

Carbon is an interstitial impurity in iron and forms a solid solution with each of α- and δ-ferrites, and also with austenite, as indicated by the α, δ, and γ single-phase fields in Figure 9.24. In the BCC α-ferrite, only small concentrations of carbon are soluble; the maximum solubility is 0.022 wt% at 727°C (1341°F). The limited solubility is explained by the shape and size of the BCC interstitial positions, which make it difficult to accommodate the carbon atoms. Even though present in relatively low concentrations, carbon significantly influences the mechanical properties of ferrite. This particular iron–carbon phase is relatively soft, may be made magnetic at temperatures below 768°C (1414°F), and has a density of 7.88 g/cm^3. Figure 9.25*a* is a photomicrograph of α-ferrite.

The austenite, or γ phase of iron, when alloyed with carbon alone, is not stable below 727°C (1341°F), as indicated in Figure 9.24. The maximum solubility of carbon in austenite, 2.14 wt%, occurs at 1147°C (2097°F). This solubility is approx-

[1] The reader may wonder why no β phase is found on the Fe–Fe_3C phase diagram, Figure 9.24 (consistent with the α, β, γ, etc. labeling scheme described previously). Early investigators observed that the ferromagnetic behavior of iron disappears at 768°C and attributed this phenomenon to a phase transformation; the "β" label was assigned to the high-temperature phase. Later it was discovered that this loss of magnetism did not result from a phase transformation (see Section 20.6) and, therefore, the presumed β phase did not exist.

imately 100 times greater than the maximum for BCC ferrite, because the FCC interstitial positions are larger (see the results of Problem 4.5), and, therefore, the strains imposed on the surrounding iron atoms are much lower. As the discussions that follow demonstrate, phase transformations involving austenite are very important in the heat treating of steels. In passing, it should be mentioned that austenite is nonmagnetic. Figure 9.25*b* shows a photomicrograph of this austenite phase.[2]

The δ-ferrite is virtually the same as α-ferrite, except for the range of temperatures over which each exists. Because the δ-ferrite is stable only at relatively high temperatures, it is of no technological importance and is not discussed further.

Cementite (Fe_3C) forms when the solubility limit of carbon in α-ferrite is exceeded below 727°C (1341°F) (for compositions within the $\alpha + Fe_3C$ phase region). As indicated in Figure 9.24, Fe_3C will also coexist with the γ phase between 727 and 1147°C (1341 and 2097°F). Mechanically, cementite is very hard and brittle; the strength of some steels is greatly enhanced by its presence.

Strictly speaking, cementite is only metastable; that is, it will remain as a compound indefinitely at room temperature. However, if heated to between 650 and 700°C (1200 and 1300°F) for several years, it will gradually change or transform into α-iron and carbon, in the form of graphite, which will remain upon subsequent cooling to room temperature. Thus, the phase diagram in Figure 9.24 is not a true equilibrium one because cementite is not an equilibrium compound. However, inasmuch as the decomposition rate of cementite is extremely sluggish, virtually all the carbon in steel will be as Fe_3C instead of graphite, and the iron–iron carbide phase diagram is, for all practical purposes, valid. As will be seen in Section 11.2, addition of silicon to cast irons greatly accelerates this cementite decomposition reaction to form graphite.

The two-phase regions are labeled in Figure 9.24. It may be noted that one eutectic exists for the iron–iron carbide system, at 4.30 wt% C and 1147°C (2097°F); for this eutectic reaction,

Eutectic reaction for the iron–iron carbide system

$$L \underset{\text{heating}}{\overset{\text{cooling}}{\rightleftharpoons}} \gamma + Fe_3C \tag{9.18}$$

the liquid solidifies to form austenite and cementite phases. Of course, subsequent cooling to room temperature will promote additional phase changes.

It may be noted that a eutectoid invariant point exists at a composition of 0.76 wt% C and a temperature of 727°C (1341°F). This eutectoid reaction may be represented by

Eutectoid reaction for the iron–iron carbide system

$$\gamma(0.76\ \text{wt\%}\ \text{C}) \underset{\text{heating}}{\overset{\text{cooling}}{\rightleftharpoons}} \alpha(0.022\ \text{wt\%}\ \text{C}) + Fe_3C(6.7\ \text{wt\%}\ \text{C}) \tag{9.19}$$

or, upon cooling, the solid γ phase is transformed into α-iron and cementite. (Eutectoid phase transformations were addressed in Section 9.14.) The eutectoid phase changes described by Equation 9.19 are very important, being fundamental to the heat treatment of steels, as explained in subsequent discussions.

Ferrous alloys are those in which iron is the prime component, but carbon as well as other alloying elements may be present. In the classification scheme of ferrous alloys based on carbon content, there are three types: iron, steel, and cast iron. Commercially pure iron contains less than 0.008 wt% C and, from the phase diagram, is composed almost exclusively of the ferrite phase at room temperature. The

[2] Annealing twins, found in alloys having the FCC crystal structure (Section 4.6), may be observed in this photomicrograph for austenite. Such do not occur in BCC alloys, which explains their absence in the ferrite micrograph of Figure 9.25*a*.

iron–carbon alloys that contain between 0.008 and 2.14 wt% C are classified as steels. In most steels the microstructure consists of both α and Fe_3C phases. Upon cooling to room temperature, an alloy within this composition range must pass through at least a portion of the γ-phase field; distinctive microstructures are subsequently produced, as discussed shortly. Although a steel alloy may contain as much as 2.14 wt% C, in practice, carbon concentrations rarely exceed 1.0 wt%. The properties and various classifications of steels are treated in Section 11.2. Cast irons are classified as ferrous alloys that contain between 2.14 and 6.70 wt% C. However, commercial cast irons normally contain less than 4.5 wt% C. These alloys are discussed further also in Section 11.2.

9.19 DEVELOPMENT OF MICROSTRUCTURE IN IRON–CARBON ALLOYS

Several of the various microstructures that may be produced in steel alloys and their relationships to the iron–iron carbon phase diagram are now discussed, and it is shown that the microstructure that develops depends on both the carbon content and heat treatment. This discussion is confined to very slow cooling of steel alloys, in which equilibrium is continuously maintained. A more detailed exploration of the influence of heat treatment on microstructure, and ultimately on the mechanical properties of steels, is contained in Chapter 10.

Phase changes that occur upon passing from the γ region into the $\alpha + Fe_3C$ phase field (Figure 9.24) are relatively complex and similar to those described for the eutectic systems in Section 9.12. Consider, for example, an alloy of eutectoid composition (0.76 wt% C) as it is cooled from a temperature within the γ phase region, say, 800°C—that is, beginning at point *a* in Figure 9.26 and moving down the

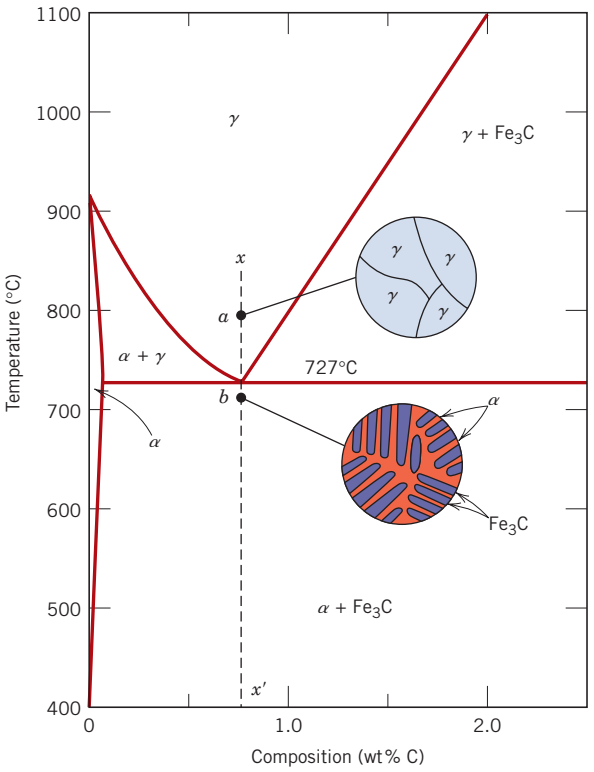

Figure 9.26 Schematic representations of the microstructures for an iron–carbon alloy of eutectoid composition (0.76 wt% C) above and below the eutectoid temperature.

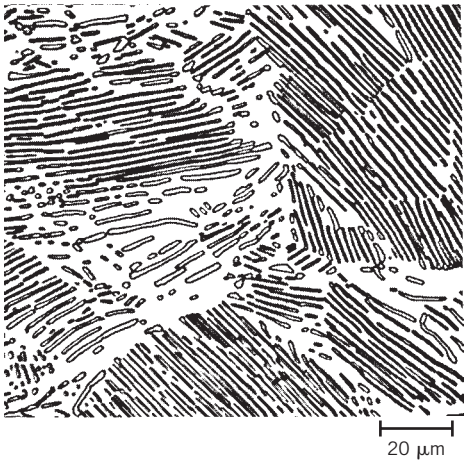

Figure 9.27 Photomicrograph of a eutectoid steel showing the pearlite microstructure consisting of alternating layers of α-ferrite (the light phase) and Fe_3C (thin layers most of which appear dark). 470×. (Reproduced with permission from *Metals Handbook,* 9th edition, Vol. 9, *Metallography and Microstructures,* American Society for Metals, Materials Park, OH, 1985.)

vertical line xx'. Initially, the alloy is composed entirely of the austenite phase having a composition of 0.76 wt% C and corresponding microstructure, also indicated in Figure 9.26. As the alloy is cooled, no changes will occur until the eutectoid temperature (727°C) is reached. Upon crossing this temperature to point b, the austenite transforms according to Equation 9.19.

The microstructure for this eutectoid steel that is slowly cooled through the eutectoid temperature consists of alternating layers or lamellae of the two phases (α and Fe_3C) that form simultaneously during the transformation. In this case, the relative layer thickness is approximately 8 to 1. This microstructure, represented schematically in Figure 9.26, point b, is called **pearlite** because it has the appearance of mother-of-pearl when viewed under the microscope at low magnifications. Figure 9.27 is a photomicrograph of a eutectoid steel showing the pearlite. The pearlite exists as grains, often termed colonies; within each colony the layers are oriented in essentially the same direction, which varies from one colony to another. The thick light layers are the ferrite phase, and the cementite phase appears as thin lamellae most of which appear dark. Many cementite layers are so thin that adjacent phase boundaries are so close together that they are indistinguishable at this magnification, and, therefore, appear dark. Mechanically, pearlite has properties intermediate between the soft, ductile ferrite and the hard, brittle cementite.

pearlite

The alternating α and Fe_3C layers in pearlite form as such for the same reason that the eutectic structure (Figures 9.13 and 9.14) forms—because the composition of the parent phase [in this case austenite (0.76 wt% C)] is different from either of the product phases [ferrite (0.022 wt% C) and cementite (6.70 wt% C)], and the phase transformation requires that there be a redistribution of the carbon by diffusion. Figure 9.28 illustrates schematically microstructural changes that accompany this eutectoid reaction; here the directions of carbon diffusion are indicated by arrows. Carbon atoms diffuse away from the 0.022 wt% ferrite regions and to the 6.70 wt% cementite layers, as the pearlite extends from the grain boundary into the unreacted austenite grain. The layered pearlite forms because carbon atoms need diffuse only minimal distances with the formation of this structure.

Furthermore, subsequent cooling of the pearlite from point b in Figure 9.26 will produce relatively insignificant microstructural changes.

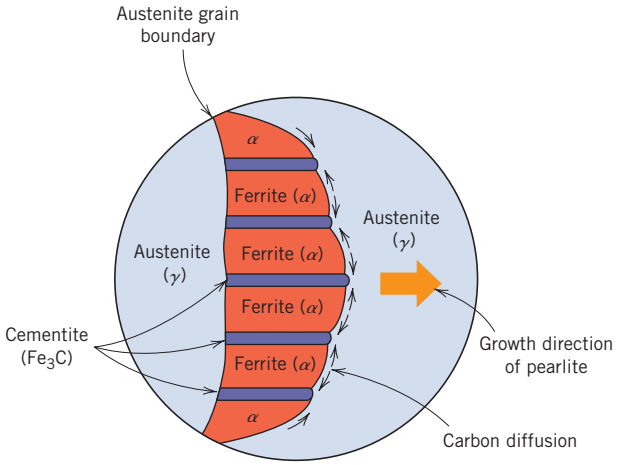

Figure 9.28 Schematic representation of the formation of pearlite from austenite; direction of carbon diffusion indicated by arrows.

Hypoeutectoid Alloys

Microstructures for iron–iron carbide alloys having other than the eutectoid composition are now explored; these are analogous to the fourth case described in Section 9.12 and illustrated in Figure 9.16 for the eutectic system. Consider a composition C_0 to the left of the eutectoid, between 0.022 and 0.76 wt% C; this is termed a **hypoeutectoid alloy.** Cooling an alloy of this composition is represented by moving down the vertical line yy' in Figure 9.29. At about 875°C, point c, the microstructure will consist entirely of grains of the γ phase, as shown

hypoeutectoid alloy

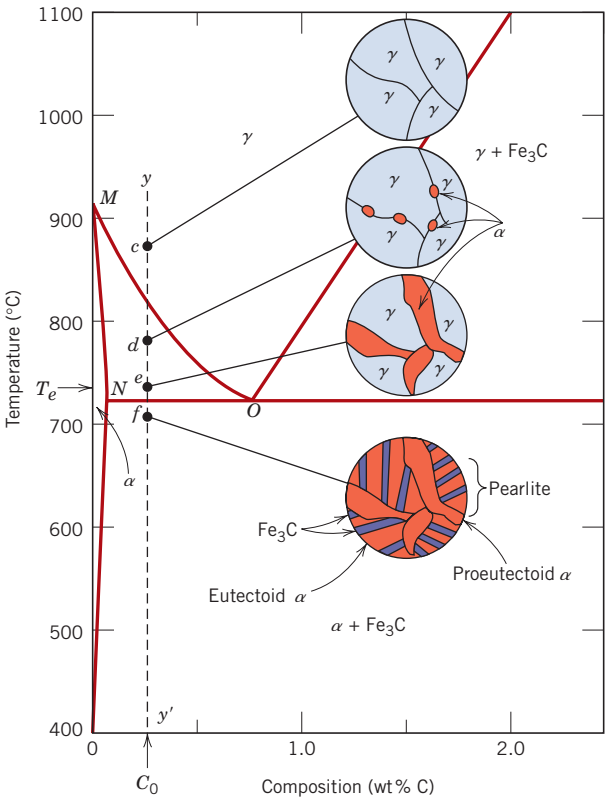

Figure 9.29 Schematic representations of the microstructures for an iron–carbon alloy of hypoeutectoid composition C_0 (containing less than 0.76 wt% C) as it is cooled from within the austenite phase region to below the eutectoid temperature.

schematically in the figure. In cooling to point d, about 775°C, which is within the $\alpha + \gamma$ phase region, both these phases will coexist as in the schematic microstructure. Most of the small α particles will form along the original γ grain boundaries. The compositions of both α and γ phases may be determined using the appropriate tie line; these compositions correspond, respectively, to about 0.020 and 0.40 wt% C.

While cooling an alloy through the $\alpha + \gamma$ phase region, the composition of the ferrite phase changes with temperature along the $\alpha - (\alpha + \gamma)$ phase boundary, line MN, becoming slightly richer in carbon. On the other hand, the change in composition of the austenite is more dramatic, proceeding along the $(\alpha + \gamma) - \gamma$ boundary, line MO, as the temperature is reduced.

Cooling from point d to e, just above the eutectoid but still in the $\alpha + \gamma$ region, will produce an increased fraction of the α phase and a microstructure similar to that also shown: the α particles will have grown larger. At this point, the compositions of the α and γ phases are determined by constructing a tie line at the temperature T_e; the α phase will contain 0.022 wt% C, whereas the γ phase will be of the eutectoid composition, 0.76 wt% C.

As the temperature is lowered just below the eutectoid, to point f, all the γ phase that was present at temperature T_e (and having the eutectoid composition) will transform to pearlite, according to the reaction in Equation 9.19. There will be virtually no change in the α phase that existed at point e in crossing the eutectoid temperature—it will normally be present as a continuous matrix phase surrounding the isolated pearlite colonies. The microstructure at point f will appear as the corresponding schematic inset of Figure 9.29. Thus the ferrite phase will be present both in the pearlite and also as the phase that formed while cooling through the $\alpha + \gamma$ phase region. The ferrite that is present in the pearlite is called *eutectoid ferrite,* whereas the other, that formed above T_e, is termed **proeutectoid** (meaning "pre- or before eutectoid") **ferrite,** as labeled in Figure 9.29. Figure 9.30 is a photomicrograph of a 0.38 wt% C steel; large, white regions correspond to the proeutectoid ferrite. For pearlite, the spacing between the α and Fe_3C layers varies

proeutectoid ferrite

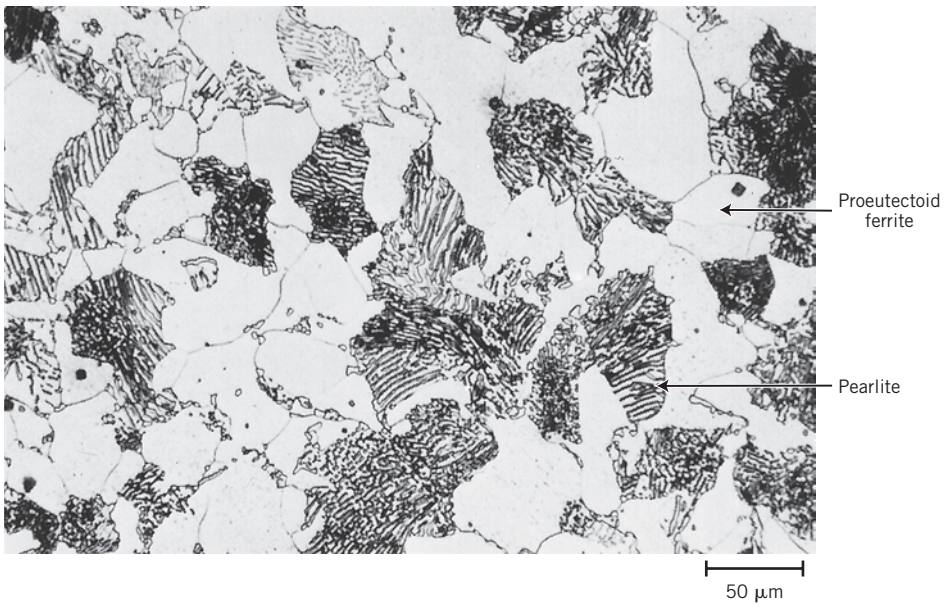

Figure 9.30 Photomicrograph of a 0.38 wt% C steel having a microstructure consisting of pearlite and proeutectoid ferrite. 635×. (Photomicrograph courtesy of Republic Steel Corporation.)

from grain to grain; some of the pearlite appears dark because the many close-spaced layers are unresolved at the magnification of the photomicrograph. Note that two microconstituents are present in this micrograph—proeutectoid ferrite and pearlite—which will appear in all hypoeutectoid iron–carbon alloys that are slowly cooled to a temperature below the eutectoid.

The relative amounts of the proeutectoid α and pearlite may be determined in a manner similar to that described in Section 9.12 for primary and eutectic microconstituents. We use the lever rule in conjunction with a tie line that extends from the $\alpha - (\alpha + Fe_3C)$ phase boundary (0.022 wt% C) to the eutectoid composition (0.76 wt% C), inasmuch as pearlite is the transformation product of austenite having this composition. For example, let us consider an alloy of composition C_0' in Figure 9.31. Thus, the fraction of pearlite, W_p, may be determined according to

Lever rule expression for computation of pearlite mass fraction (composition C_0', Figure 9.31)

$$W_p = \frac{T}{T + U}$$

$$= \frac{C_0' - 0.022}{0.76 - 0.022} = \frac{C_0' - 0.022}{0.74} \tag{9.20}$$

Furthermore, the fraction of proeutectoid α, $W_{\alpha'}$, is computed as follows:

Lever rule expression for computation of proeutectoid ferrite mass fraction

$$W_{\alpha'} = \frac{U}{T + U}$$

$$= \frac{0.76 - C_0'}{0.76 - 0.022} = \frac{0.76 - C_0'}{0.74} \tag{9.21}$$

Of course, fractions of both total α (eutectoid and proeutectoid) and cementite are determined using the lever rule and a tie line that extends across the entirety of the $\alpha + Fe_3C$ phase region, from 0.022 to 6.70 wt% C.

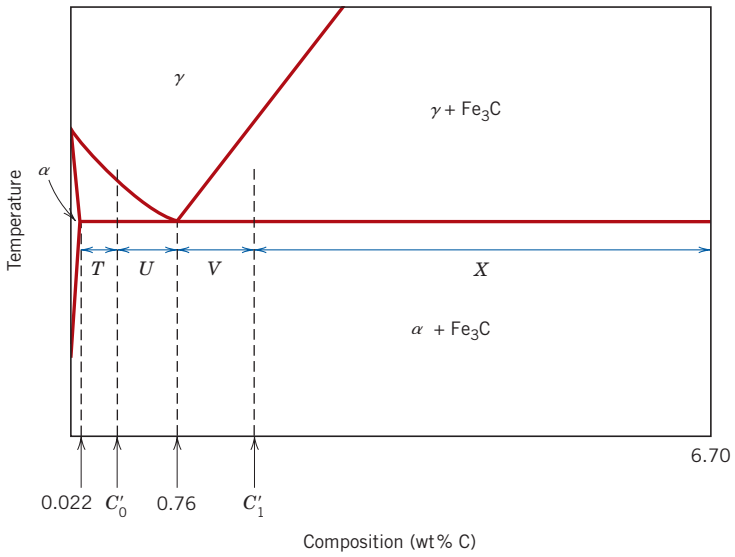

Figure 9.31 A portion of the Fe–Fe_3C phase diagram used in computations for relative amounts of proeutectoid and pearlite microconstituents for hypoeutectoid C_0' and hypereutectoid C_1' compositions.

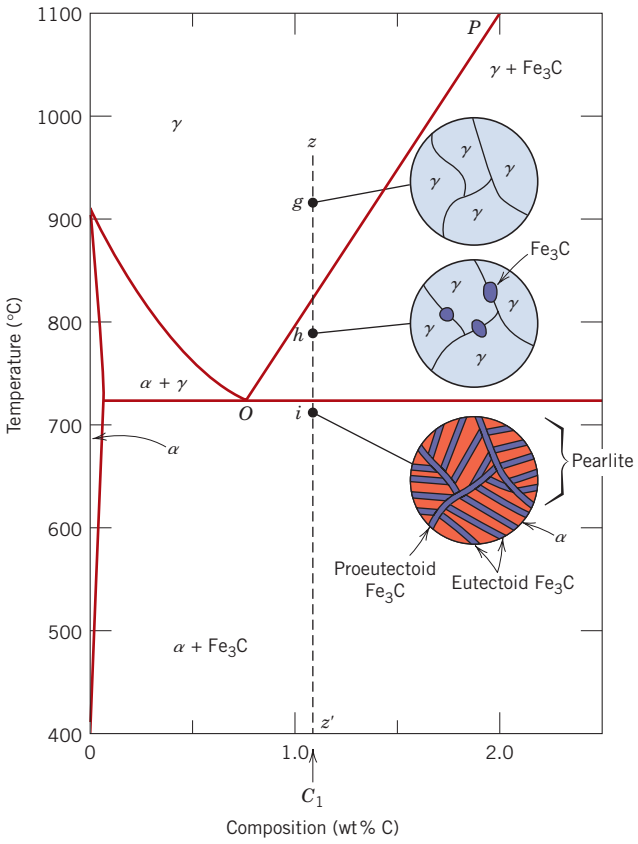

Figure 9.32 Schematic representations of the microstructures for an iron–carbon alloy of hypereutectoid composition C_1 (containing between 0.76 and 2.14 wt% C), as it is cooled from within the austenite phase region to below the eutectoid temperature.

Hypereutectoid Alloys

hypereutectoid alloy

Analogous transformations and microstructures result for **hypereutectoid alloys,** those containing between 0.76 and 2.14 wt% C, which are cooled from temperatures within the γ phase field. Consider an alloy of composition C_1 in Figure 9.32 that, upon cooling, moves down the line zz'. At point g only the γ phase will be present with a composition of C_1; the microstructure will appear as shown, having only γ grains. Upon cooling into the $\gamma + Fe_3C$ phase field—say, to point h—the cementite phase will begin to form along the initial γ grain boundaries, similar to the α phase in Figure 9.29, point d. This cementite is called **proeutectoid cementite**—that which forms before the eutectoid reaction. Of course, the cementite composition remains constant (6.70 wt% C) as the temperature changes. However, the composition of the austenite phase will move along line PO toward the eutectoid. As the temperature is lowered through the eutectoid to point i, all remaining austenite of eutectoid composition is converted into pearlite; thus, the resulting microstructure consists of pearlite and proeutectoid cementite as microconstituents (Figure 9.32). In the photomicrograph of a 1.4 wt% C steel (Figure 9.33), note that the proeutectoid cementite appears light. Because it has much the same appearance as proeutectoid ferrite (Figure 9.30), there is some difficulty in distinguishing between hypoeutectoid and hypereutectoid steels on the basis of microstructure.

proeutectoid cementite

Relative amounts of both pearlite and proeutectoid Fe_3C microconstituents may be computed for hypereutectoid steel alloys in a manner analogous to that for hypoeutectoid materials; the appropriate tie line extends between 0.76 and 6.70

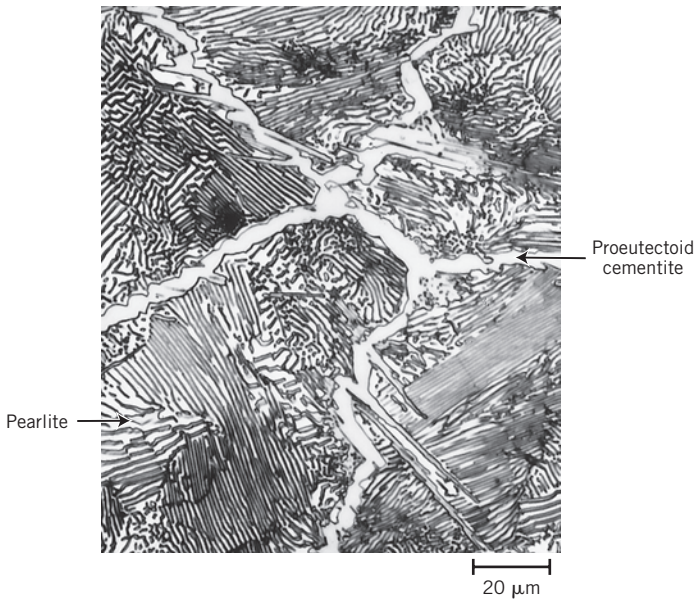

Figure 9.33 Photomicrograph of a 1.4 wt% C steel having a microstructure consisting of a white proeutectoid cementite network surrounding the pearlite colonies. 1000×. (Copyright 1971 by United States Steel Corporation.)

wt% C. Thus, for an alloy having composition C_1' in Figure 9.31, fractions of pearlite W_p and proeutectoid cementite $W_{Fe_3C'}$ are determined from the following lever rule expressions:

$$W_p = \frac{X}{V + X} = \frac{6.70 - C_1'}{6.70 - 0.76} = \frac{6.70 - C_1'}{5.94} \tag{9.22}$$

and

$$W_{Fe_3C'} = \frac{V}{V + X} = \frac{C_1' - 0.76}{6.70 - 0.76} = \frac{C_1' - 0.76}{5.94} \tag{9.23}$$

Concept Check 9.8

Briefly explain why a proeutectoid phase (ferrite or cementite) forms along austenite grain boundaries. *Hint*: Consult Section 4.6.

[*The answer may be found at www.wiley.com/college/callister (Student Companion Site).*]

EXAMPLE PROBLEM 9.4

Determination of Relative Amounts of Ferrite, Cementite, and Pearlite Microconstituents

For a 99.65 wt% Fe–0.35 wt% C alloy at a temperature just below the eutectoid, determine the following:

(a) The fractions of total ferrite and cementite phases

(b) The fractions of the proeutectoid ferrite and pearlite

(c) The fraction of eutectoid ferrite

Solution

(a) This part of the problem is solved by application of the lever rule expressions employing a tie line that extends all the way across the $\alpha + Fe_3C$ phase field. Thus, C_0' is 0.35 wt% C, and

$$W_\alpha = \frac{6.70 - 0.35}{6.70 - 0.022} = 0.95$$

and

$$W_{Fe_3C} = \frac{0.35 - 0.022}{6.70 - 0.022} = 0.05$$

(b) The fractions of proeutectoid ferrite and pearlite are determined by using the lever rule and a tie line that extends only to the eutectoid composition (i.e., Equations 9.20 and 9.21). Or

$$W_p = \frac{0.35 - 0.022}{0.76 - 0.022} = 0.44$$

and

$$W_{\alpha'} = \frac{0.76 - 0.35}{0.76 - 0.022} = 0.56$$

(c) All ferrite is either as proeutectoid or eutectoid (in the pearlite). Therefore, the sum of these two ferrite fractions will equal the fraction of total ferrite; that is,

$$W_{\alpha'} + W_{\alpha e} = W_\alpha$$

where $W_{\alpha e}$ denotes the fraction of the total alloy that is eutectoid ferrite. Values for W_α and $W_{\alpha'}$ were determined in parts (a) and (b) as 0.95 and 0.56, respectively. Therefore,

$$W_{\alpha e} = W_\alpha - W_{\alpha'} = 0.95 - 0.56 = 0.39$$

Nonequilibrium Cooling

In this discussion on the microstructural development of iron–carbon alloys it has been assumed that, upon cooling, conditions of metastable equilibrium[3] have been continuously maintained; that is, sufficient time has been allowed at each new temperature for any necessary adjustment in phase compositions and relative amounts as predicted from the Fe–Fe_3C phase diagram. In most situations these cooling rates are impractically slow and really unnecessary; in fact, on many occasions nonequilibrium conditions are desirable. Two nonequilibrium effects of practical importance are (1) the occurrence of phase changes or transformations at temperatures other than those predicted by phase boundary lines on the phase diagram, and (2) the

[3] The term *metastable equilibrium* is used in this discussion inasmuch as Fe_3C is only a metastable compound.

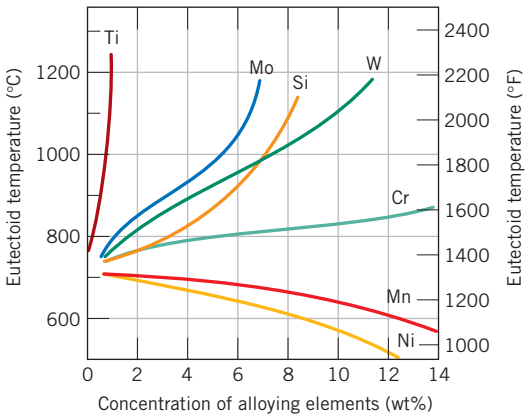

Figure 9.34 The dependence of eutectoid temperature on alloy concentration for several alloying elements in steel. (From Edgar C. Bain, *Functions of the Alloying Elements in Steel,* American Society for Metals, 1939, p. 127.)

existence at room temperature of nonequilibrium phases that do not appear on the phase diagram. Both are discussed in the next chapter.

9.20 THE INFLUENCE OF OTHER ALLOYING ELEMENTS

Additions of other alloying elements (Cr, Ni, Ti, etc.) bring about rather dramatic changes in the binary iron–iron carbide phase diagram, Figure 9.24. The extent of these alterations of the positions of phase boundaries and the shapes of the phase fields depends on the particular alloying element and its concentration. One of the important changes is the shift in position of the eutectoid with respect to temperature and to carbon concentration. These effects are illustrated in Figures 9.34 and 9.35, which plot the eutectoid temperature and eutectoid composition (in wt% C) as a function of concentration for several other alloying elements. Thus, other alloy additions alter not only the temperature of the eutectoid reaction but also the relative fractions of pearlite and the proeutectoid phase that form. Steels are normally alloyed for other reasons, however—usually either to improve their corrosion resistance or to render them amenable to heat treatment (see Section 11.8).

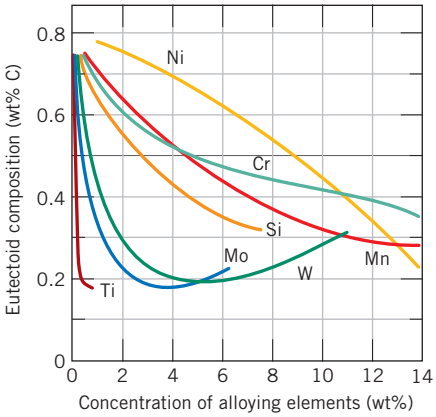

Figure 9.35 The dependence of eutectoid composition (wt% C) on alloy concentration for several alloying elements in steel. (From Edgar C. Bain, *Functions of the Alloying Elements in Steel,* American Society for Metals, 1939, p. 127.)

SUMMARY

Introduction

- Equilibrium phase diagrams are a convenient and concise way of representing the most stable relationships between phases in alloy systems.

Phases

- A phase is some portion of a body of material throughout which the physical and chemical characteristics are homogeneous.

Microstructure

- Three microstructural characteristics that are important for multiphase alloys are
  - The number of phases present
  - The relative proportions of the phases
  - The manner in which the phases are arranged
- Three factors affect the microstructure of an alloy:
  - What alloying elements are present
  - The concentrations of these alloying elements
  - The heat treatment of the alloy

Phase Equilibria

- A system at equilibrium is in its most stable state—that is, its phase characteristics do not change over time. Thermodynamically, the condition for phase equilibrium is that the free energy of a system is a minimum for some set combination of temperature, pressure, and composition.
- Metastable systems are nonequilibrium ones that persist indefinitely and experience imperceptible changes with time.

One-Component (or Unary) Phase Diagrams

- For one-component phase diagrams logarithm of pressure is plotted versus temperature; solid-, liquid-, and vapor-phase regions are found on this type of diagram.

Binary Phase Diagrams

- For binary systems, temperature and composition are variables, whereas external pressure is held constant. Areas, or phase regions, are defined on these temperature-versus-composition plots within which either one or two phases exist.

Binary Isomorphous Systems

- Isomorphous diagrams are those for which there is complete solubility in the solid phase; the copper–nickel system (Figure 9.3*a*) displays this behavior.

Interpretation of Phase Diagrams

- For an alloy of specified composition, at a known temperature, and that is at equilibrium, the following may be determined:
  - What phase(s) is (are) present—from the location of the temperature–composition point on the phase diagram.
  - Phase composition(s)—for the two-phase situation a horizontal tie line is employed.
  - Phase mass fraction(s)—the lever rule [which utilizes tie line segment lengths (Equations 9.1 and 9.2)] is used in two-phase regions.

Binary Eutectic Systems

- In a eutectic reaction, as found in some alloy systems, a liquid phase transforms isothermally to two different solid phases upon cooling (i.e., $L \rightarrow \alpha + \beta$). Such a reaction is noted on the copper–silver and lead–tin phase diagrams (Figures 9.7 and 9.8, respectively).
- The solubility limit at some temperature corresponds to the maximum concentration of one component that will go into solution in a specific phase. For a binary eutectic system, solubility limits are to be found along solidus and solvus phase boundaries.

Development of Microstructure in Eutectic Alloys

- The solidification of an alloy (liquid) of eutectic composition yields a microstructure consisting of layers of the two solid phases that alternate.
- A primary (or pre-eutectic) phase as well as the layered eutectic structure will be the solidification products for all compositions (other than the eutectic) that lie along the eutectic isotherm.
- Mass fractions of the primary phase and eutectic microconstituent may be computed using the lever rule and a tie line that extends to the eutectic composition (e.g., Equations 9.10 and 9.11).

Equilibrium Diagrams Having Intermediate Phases or Compounds

- Other equilibrium diagrams are more complex in that they may have phases/solid solutions/compounds that do not lie at the concentration (i.e., horizontal) extremities on the diagram. These include intermediate solid solutions and intermetallic compounds.
- In addition to the eutectic, other reactions involving three phases may occur at invariant points on a phase diagram:
  - For a eutectoid reaction, upon cooling, one solid phase transforms into two other solid phases (e.g., $\alpha \rightarrow \beta + \gamma$).
  - For a peritectic reaction, upon cooling, a liquid and one solid phase transform to another solid phase (e.g., $L + \alpha \rightarrow \beta$).
- A transformation wherein there is no change in composition for the phases involved is congruent.

The Gibbs Phase Rule

- The Gibbs phase rule is a simple equation (Equation 9.16 in its most general form) that relates the number of phases present in a system at equilibrium with the number of degrees of freedom, the number of components, and the number of noncompositional variables.

The Iron–Iron Carbide (Fe–Fe_3C) Phase Diagram

- Important phases found on the iron–iron carbide phase diagram (Figure 9.24) are α–ferrite (BCC), γ-austenite (FCC), and the intermetallic compound iron carbide [or cementite (Fe_3C)].
- On the basis of composition, ferrous alloys fall into three classifications:
  - Irons (<0.008 wt% C)
  - Steels (0.008 wt% C to 2.14 wt% C)
  - Cast irons (>2.14 wt% C)

Development of Microstructure in Iron–Carbon Alloys

- The development of microstructure for many iron–carbon alloys and steels depends on a eutectoid reaction in which the austenite phase of composition 0.76 wt% C transforms isothermally (at 727°C) to α-ferrite (0.022 wt% C) and cementite (i.e., $\gamma \rightarrow \alpha + Fe_3C$).
- The microstructural product of an iron–carbon alloy of eutectoid composition is pearlite, a microconstituent consisting of alternating layers of ferrite and cementite.
- The microstructures of alloys having carbon contents less than the eutectoid (i.e., hypoeutectoid alloys) are composed of a proeutectoid ferrite phase in addition to pearlite.
- Pearlite and proeutectoid cementite constitute the microconstituents for hypereutectoid alloys—those with carbon contents in excess of the eutectoid composition.
- Mass fractions of a proeutectoid phase (ferrite or cementite) and pearlite may be computed using the lever rule and a tie line that extends to the eutectoid composition (0.76 wt% C) [e.g., Equations 9.20 and 9.21 (for hypoeutectoid alloys) and Equations 9.22 and 9.23 (for hypereutectoid alloys)].

Equation Summary

Equation Number	*Equation*	*Solving for*	*Page Number*
9.1b	$W_L = \dfrac{C_\alpha - C_0}{C_\alpha - C_L}$	Mass fraction of liquid phase, binary isomorphous system	291
9.2b	$W_\alpha = \dfrac{C_0 - C_L}{C_\alpha - C_L}$	Mass fraction of α solid-solution phase, binary isomorphous system	291
9.5	$V_\alpha = \dfrac{v_\alpha}{v_\alpha + v_\beta}$	Volume fraction of α phase	293
9.6a	$V_\alpha = \dfrac{\dfrac{W_\alpha}{\rho_\alpha}}{\dfrac{W_\alpha}{\rho_\alpha} + \dfrac{W_\beta}{\rho_\beta}}$	For α phase, conversion of mass fraction to volume fraction	293
9.7a	$W_\alpha = \dfrac{V_\alpha \rho_\alpha}{V_\alpha \rho_\alpha + V_\beta \rho_\beta}$	For α phase, conversion of volume fraction to mass fraction	293
9.10	$W_e = \dfrac{P}{P + Q}$	Mass fraction of eutectic microconstituent for binary eutectic system (per Figure 9.18)	310
9.11	$W_{\alpha'} = \dfrac{Q}{P + Q}$	Mass fraction of primary α microconstituent for binary eutectic system (per Figure 9.18)	310
9.12	$W_\alpha = \dfrac{Q + R}{P + Q + R}$	Mass fraction of total α phase for a binary eutectic system (per Figure 9.18)	310
9.13	$W_\beta = \dfrac{P}{P + Q + R}$	Mass fraction of β phase for a binary eutectic system (per Figure 9.18)	311
9.16	$P + F = C + N$	Gibbs phase rule (general form)	316

9.20	$W_p = \dfrac{C_0' - 0.022}{0.74}$	For a *hypo*eutectoid Fe–C alloy, the mass fraction of pearlite (per Figure 9.31)	326
9.21	$W_{\alpha'} = \dfrac{0.76 - C_0'}{0.74}$	For a *hypo*eutectoid Fe–C alloy, the mass fraction of proeutectoid α ferrite phase (per Figure 9.31)	326
9.22	$W_p = \dfrac{6.70 - C_1'}{5.94}$	For a *hyper*eutectoid Fe–C alloy, the mass fraction of pearlite (per Figure 9.31)	328
9.23	$W_{Fe_3C'} = \dfrac{C_1' - 0.76}{5.94}$	For a *hyper*eutectoid Fe–C alloy, the mass fraction of proeutectoid Fe_3C (per Figure 9.31)	328

List of Symbols

Symbol	*Meaning*
C (Gibbs phase rule)	Number of components in a system
C_0	Composition of alloy (in terms of one of the components)
C_0'	Composition of a hypoeutectoid alloy (in weight percent carbon)
C_1'	Composition of a hypereutectoid alloy (in weight percent carbon)
F	Number of externally controlled variables that must be specified to completely define the state of a system
N	Number of noncompositional variables for a system
P, Q, R	Lengths of tie–line segments
P (Gibbs phase rule)	Number of phases present in a given system
v_α, v_β	Volumes of α and β phases
ρ_α, ρ_β	Densities of α and β phases

Processing/Structure/Properties/Performance Summary

For iron–carbon alloys (i.e., steels), an understanding of microstructures that develop during relatively slow rates of cooling (i.e., pearlite and a proeutectoid phase) is facilitated by the iron–iron carbide phase diagram. Other concepts in this chapter were presented as a prelude to the introduction of this diagram—the concepts of a phase, phase equilibrium, metastability, and the eutectoid reaction. In Chapter 10 we explore yet other microstructures that form when iron–carbon alloys are cooled from elevated temperatures at more rapid rates. These concepts are summarized in the following diagram:

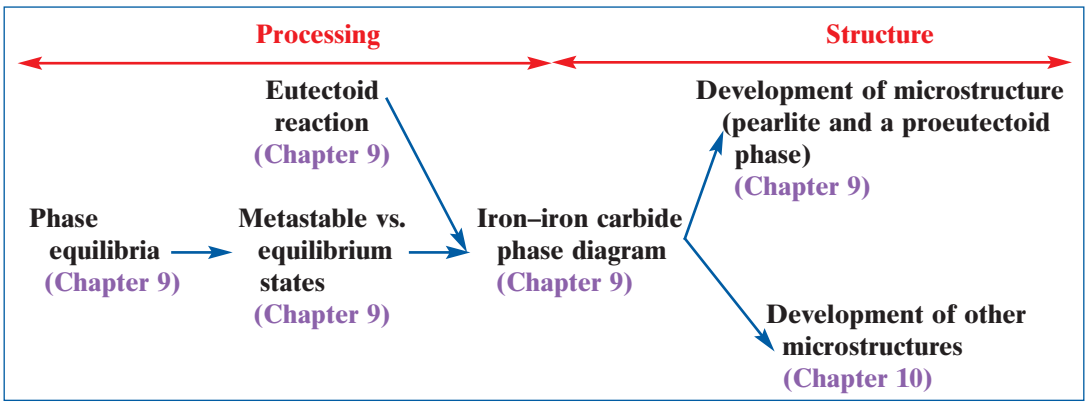

Important Terms and Concepts

austenite
cementite
component
congruent transformation
equilibrium
eutectic phase
eutectic reaction
eutectic structure
eutectoid reaction
ferrite
free energy
Gibbs phase rule
hypereutectoid alloy
hypoeutectoid alloy
intermediate solid solution
intermetallic compound
invariant point
isomorphous
lever rule
liquidus line
metastable
microconstituent
pearlite
peritectic reaction
phase
phase diagram
phase equilibrium
primary phase
proeutectoid cementite
proeutectoid ferrite
solidus line
solubility limit
solvus line
system
terminal solid solution
tie line

REFERENCES

ASM Handbook, Vol. 3, *Alloy Phase Diagrams,* ASM International, Materials Park, OH, 1992.

ASM Handbook, Vol. 9, *Metallography and Microstructures,* ASM International, Materials Park, OH, 2004.

Massalski, T. B., H. Okamoto, P. R. Subramanian, and L. Kacprzak (Editors), *Binary Phase Diagrams,* 2nd edition, ASM International, Materials Park, OH, 1990. Three volumes. Also on CD-ROM with updates.

Okamoto, H., *Desk Handbook: Phase Diagrams for Binary Alloys,* ASM International, Materials Park, OH, 2000.

Villars, P., A. Prince, and H. Okamoto (Editors), *Handbook of Ternary Alloy Phase Diagrams,* ASM International, Materials Park, OH, 1995. Ten volumes. Also on CD-ROM.

QUESTIONS AND PROBLEMS

Solubility Limit

9.1 Consider the sugar–water phase diagram of Figure 9.1.

(a) How much sugar will dissolve in 1500 g of water at 90°C (194°F)?

(b) If the saturated liquid solution in part (a) is cooled to 20°C (68°F), some of the sugar will precipitate out as a solid. What will be the composition of the saturated liquid solution (in wt% sugar) at 20°C?

(c) How much of the solid sugar will come out of solution upon cooling to 20°C?

9.2 At 500°C (930°F), what is the maximum solubility **(a)** of Cu in Ag? **(b)** Of Ag in Cu?

Microstructure

9.3 Cite three variables that determine the microstructure of an alloy.

Phase Equilibria

9.4 What thermodynamic condition must be met for a state of equilibrium to exist?

One-Component (or Unary) Phase Diagrams

9.5 Consider a specimen of ice that is at −10°C and 1 atm pressure. Using Figure 9.2, the pressure–temperature phase diagram for H_2O, determine the pressure to which the specimen must be raised or lowered to cause it **(a)** to melt, and **(b)** to sublime.

9.6 At a pressure of 0.01 atm, determine **(a)** the melting temperature for ice, and **(b)** the boiling temperature for water.

Binary Isomorphous Systems

9.7 Given here are the solidus and liquidus temperatures for the germanium–silicon system. Construct the phase diagram for this system and label each region.

Composition (wt% Si)	*Solidus Temperature (°C)*	*Liquidus Temperature (°C)*
0	938	938
10	1005	1147
20	1065	1226
30	1123	1278
40	1178	1315
50	1232	1346
60	1282	1367
70	1326	1385
80	1359	1397
90	1390	1408
100	1414	1414

Interpretation of Phase Diagrams

9.8 Cite the phases that are present and the phase compositions for the following alloys:

(a) 90 wt% Zn–10 wt% Cu at 400°C (750°F)

(b) 75 wt% Sn–25 wt% Pb at 175°C (345°F)

(c) 55 wt% Ag–45 wt% Cu at 900°C (1650°F)

(d) 30 wt% Pb–70 wt% Mg at 425°C (795°F)

(e) 2.12 kg Zn and 1.88 kg Cu at 500°C (930°F)

(f) 37 lb_m Pb and 6.5 lb_m Mg at 400°C (750°F)

(g) 8.2 mol Ni and 4.3 mol Cu at 1250°C (2280°F)

(h) 4.5 mol Sn and 0.45 mol Pb at 200°C (390°F)

9.9 Is it possible to have a copper–nickel alloy that, at equilibrium, consists of a liquid phase of composition 20 wt% Ni–80 wt% Cu and also an α phase of composition 37 wt% Ni–63 wt% Cu? If so, what will be the approximate temperature of the alloy? If this is not possible, explain why.

9.10 Is it possible to have a copper–zinc alloy that, at equilibrium, consists of an ϵ phase of composition 80 wt% Zn–20 wt% Cu, and also a liquid phase of composition 95 wt% Zn–5 wt% Cu? If so, what will be the approximate temperature of the alloy? If this is not possible, explain why.

9.11 A copper–nickel alloy of composition 70 wt% Ni–30 wt% Cu is slowly heated from a temperature of 1300°C (2370°F).

(a) At what temperature does the first liquid phase form?

(b) What is the composition of this liquid phase?

(c) At what temperature does complete melting of the alloy occur?

(d) What is the composition of the last solid remaining prior to complete melting?

9.12 A 50 wt% Pb–50 wt% Mg alloy is slowly cooled from 700°C (1290°F) to 400°C (750°F).

(a) At what temperature does the first solid phase form?

(b) What is the composition of this solid phase?

(c) At what temperature does the liquid solidify?

(d) What is the composition of this last remaining liquid phase?

9.13 For an alloy of composition 74 wt% Zn–26 wt% Cu, cite the phases present and their compositions at the following temperatures: 850°C, 750°C, 680°C, 600°C, and 500°C.

9.14 Determine the relative amounts (in terms of mass fractions) of the phases for the alloys and temperatures given in Problem 9.8.

9.15 A 1.5-kg specimen of a 90 wt% Pb–10 wt% Sn alloy is heated to 250°C (480°F); at this temperature it is entirely an α-phase solid solution (Figure 9.8). The alloy is to be melted to the extent that 50% of the specimen is liquid, the remainder being the α phase. This may be accomplished either by heating the alloy or changing its composition while holding the temperature constant.

(a) To what temperature must the specimen be heated?

(b) How much tin must be added to the 1.5-kg specimen at 250°C to achieve this state?

9.16 A magnesium–lead alloy of mass 5.5 kg consists of a solid α phase that has a composition just slightly below the solubility limit at 200°C (390°F).

(a) What mass of lead is in the alloy?

(b) If the alloy is heated to 350°C (660°F), how much more lead may be dissolved in the α phase without exceeding the solubility limit of this phase?

9.17 A 90 wt% Ag–10 wt% Cu alloy is heated to a temperature within the β + liquid phase region. If the composition of the liquid phase is 85 wt% Ag, determine:

(a) The temperature of the alloy

(b) The composition of the β phase

(c) The mass fractions of both phases

9.18 A 30 wt% Sn–70 wt% Pb alloy is heated to a temperature within the α + liquid phase region. If the mass fraction of each phase is 0.5, estimate:

(a) The temperature of the alloy

(b) The compositions of the two phases

9.19 For alloys of two hypothetical metals A and B, there exist an α, A-rich phase and a β, B-rich phase. From the mass fractions of both phases for two different alloys provided in the following table (which are at the same temperature), determine the composition of the phase boundary (or solubility limit) for both α and β phases at this temperature.

Alloy Composition	*Fraction α Phase*	*Fraction β Phase*
60 wt% A–40 wt% B	0.57	0.43
30 wt% A–70 wt% B	0.14	0.86

9.20 A hypothetical A–B alloy of composition 55 wt% B–45 wt% A at some temperature is found to consist of mass fractions of 0.5 for both α and β phases. If the composition of the β phase is 90 wt% B–10 wt% A, what is the composition of the α phase?

9.21 Is it possible to have a copper–silver alloy of composition 50 wt% Ag–50 wt% Cu that, at equilibrium, consists of α and β phases having mass fractions $W_\alpha = 0.60$ and $W_\beta = 0.40$? If so, what will be the approximate temperature of the alloy? If such an alloy is not possible, explain why.

9.22 For 11.20 kg of a magnesium–lead alloy of composition 30 wt% Pb–70 wt% Mg, is it possible, at equilibrium, to have α and Mg_2Pb phases having respective masses of 7.39 kg and 3.81 kg? If so, what will be the approximate temperature of the alloy? If such an alloy is not possible, explain why.

9.23 Derive Equations 9.6a and 9.7a, which may be used to convert mass fraction to volume fraction, and vice versa.

9.24 Determine the relative amounts (in terms of volume fractions) of the phases for the alloys and temperatures given in Problem 9.8a, b, and c. The following table gives the approximate densities of the various metals at the alloy temperatures:

Metal	*Temperature (°C)*	*Density (g/cm³)*
Ag	900	9.97
Cu	400	8.77
Cu	900	8.56
Pb	175	11.20
Sn	175	7.22
Zn	400	6.83

Development of Microstructure in Isomorphous Alloys

9.25 **(a)** Briefly describe the phenomenon of coring and why it occurs.

(b) Cite one undesirable consequence of coring.

Mechanical Properties of Isomorphous Alloys

9.26 It is desirable to produce a copper–nickel alloy that has a minimum noncold-worked tensile strength of 350 MPa (50,750 psi) and a ductility of at least 48%EL. Is such an alloy possible? If so, what must be its composition? If this is not possible, then explain why.

Binary Eutectic Systems

9.27 A 45 wt% Pb–55 wt% Mg alloy is rapidly quenched to room temperature from an elevated temperature in such a way that the high-temperature microstructure is preserved. This microstructure is found to consist of the α phase and Mg_2Pb, having respective mass fractions of 0.65 and 0.35. Determine the approximate temperature from which the alloy was quenched.

Development of Microstructure in Eutectic Alloys

9.28 Briefly explain why, upon solidification, an alloy of eutectic composition forms a microstructure consisting of alternating layers of the two solid phases.

9.29 What is the difference between a phase and a microconstituent?

9.30 Is it possible to have a copper–silver alloy in which the mass fractions of primary β and total β are 0.68 and 0.925, respectively, at 775°C (1425°F)? Why or why not?

9.31 For 6.70 kg of a magnesium–lead alloy, is it possible to have the masses of primary α and total α of 4.23 kg and 6.00 kg, respectively, at 460°C (860°F)? Why or why not?

9.32 For a copper–silver alloy of composition 25 wt% Ag–75 wt% Cu and at 775°C (1425°F), do the following:

(a) Determine the mass fractions of α and β phases.

(b) Determine the mass fractions of primary α and eutectic microconstituents.

(c) Determine the mass fraction of eutectic α.

9.33 The microstructure of a lead–tin alloy at 180°C (355°F) consists of primary β and eutectic structures. If the mass fractions of these two microconstituents are 0.57 and 0.43, respectively, determine the composition of the alloy.

9.34 Consider the hypothetical eutectic phase diagram for metals A and B, which is similar to that for the lead–tin system, Figure 9.8. Assume that (1) α and β phases exist at the A and B extremities of the phase diagram, respectively; (2) the eutectic composition is 47 wt% B–53 wt% A; and (3) the composition of the β phase at the eutectic temperature is 92.6 wt% B–7.4 wt% A. Determine the composition of an alloy that will yield primary α and total α mass fractions of 0.356 and 0.693, respectively.

9.35 For an 85 wt% Pb–15 wt% Mg alloy, make schematic sketches of the microstructure that would be observed for conditions of very slow cooling at the following temperatures: 600°C (1110°F), 500°C (930°F), 270°C (520°F), and 200°C (390°F). Label all phases and indicate their approximate compositions.

9.36 For a 68 wt% Zn–32 wt% Cu alloy, make schematic sketches of the microstructure that would be observed for conditions of very slow cooling at the following temperatures: 1000°C (1830°F), 760°C (1400°F), 600°C (1110°F), and 400°C (750°F). Label all phases and indicate their approximate compositions.

9.37 For a 30 wt% Zn–70 wt% Cu alloy, make schematic sketches of the microstructure that would be observed for conditions of very slow cooling at the following temperatures: 1100°C (2010°F), 950°C (1740°F), 900°C (1650°F), and 700°C (1290°F). Label all phases and indicate their approximate compositions.

9.38 On the basis of the photomicrograph (i.e., the relative amounts of the microconstituents) for the lead–tin alloy shown in Figure 9.17 and the Pb–Sn phase diagram (Figure 9.8), estimate the composition of the alloy, and then compare this estimate with the composition given in the figure legend of Figure 9.17. Make the following assumptions: (1) The area fraction of each phase and microconstituent in the photomicrograph is equal to its volume fraction; (2) the densities of the α and β phases as well as the eutectic structure are 11.2, 7.3, and 8.7 g/cm^3, respectively; and (3) this photomicrograph represents the equilibrium microstructure at 180°C (355°F).

9.39 The room-temperature tensile strengths of pure lead and pure tin are 16.8 MPa and 14.5 MPa, respectively.

(a) Make a schematic graph of the room-temperature tensile strength versus composition for all compositions between pure lead and pure tin. (*Hint:* you may want to consult Sections 9.10 and 9.11, as well as Equation 9.24 in Problem 9.64.)

(b) On this same graph schematically plot tensile strength versus composition at 150°C.

(c) Explain the shapes of these two curves, as well as any differences between them.

Equilibrium Diagrams Having Intermediate Phases or Compounds

9.40 Two intermetallic compounds, AB and AB_2, exist for elements A and B. If the compositions for AB and AB_2 are 34.3 wt% A–65.7 wt% B and 20.7 wt% A–79.3 wt% B, respectively, and element A is potassium, identify element B.

Congruent Phase Transformations

Eutectoid and Peritectic Reactions

9.41 What is the principal difference between congruent and incongruent phase transformations?

9.42 Figure 9.36 is the aluminum–neodymium phase diagram, for which only single–phase regions are labeled. Specify temperature–composition points at which all eutectics, eutectoids, peritectics, and congruent phase transformations occur. Also, for each, write the reaction upon cooling.

9.43 Figure 9.37 is a portion of the titanium–copper phase diagram for which only single-phase regions are labeled. Specify all temperature–

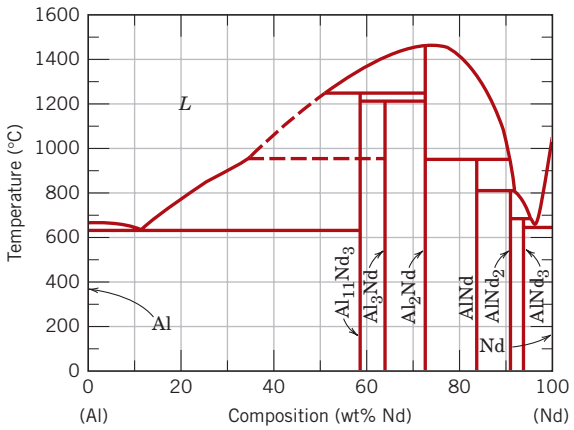

Figure 9.36 The aluminum–neodymium phase diagram. (Adapted from *ASM Handbook,* Vol. 3, *Alloy Phase Diagrams,* H. Baker, Editor, 1992. Reprinted by permission of ASM International, Materials Park, OH.)

composition points at which eutectics, eutectoids, peritectics, and congruent phase transformations occur. Also, for each, write the reaction upon cooling.

9.44 Construct the hypothetical phase diagram for metals A and B between temperatures of 600°C and 1000°C given the following information:

- The melting temperature of metal A is 940°C.
- The solubility of B in A is negligible at all temperatures.
- The melting temperature of metal B is 830°C.
- The maximum solubility of A in B is 12 wt% A, which occurs at 700°C.
- At 600°C, the solubility of A in B is 8 wt% A.
- One eutectic occurs at 700°C and 75 wt% B–25 wt% A.
- A second eutectic occurs at 730°C and 60 wt% B–40 wt% A.
- A third eutectic occurs at 755°C and 40 wt% B–60 wt% A.

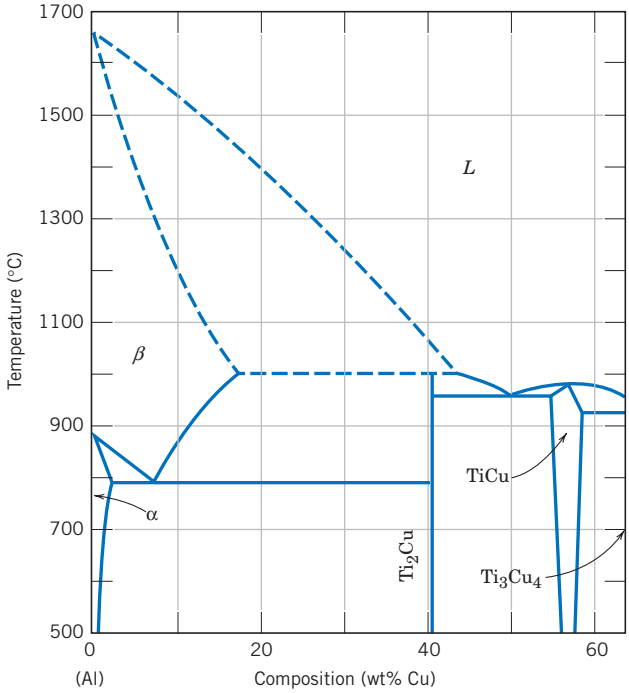

Figure 9.37 The titanium–copper phase diagram. (Adapted from *Phase Diagrams of Binary Titanium Alloys,* J. L. Murray, Editor, 1987. Reprinted by permission of ASM International, Materials Park, OH.)

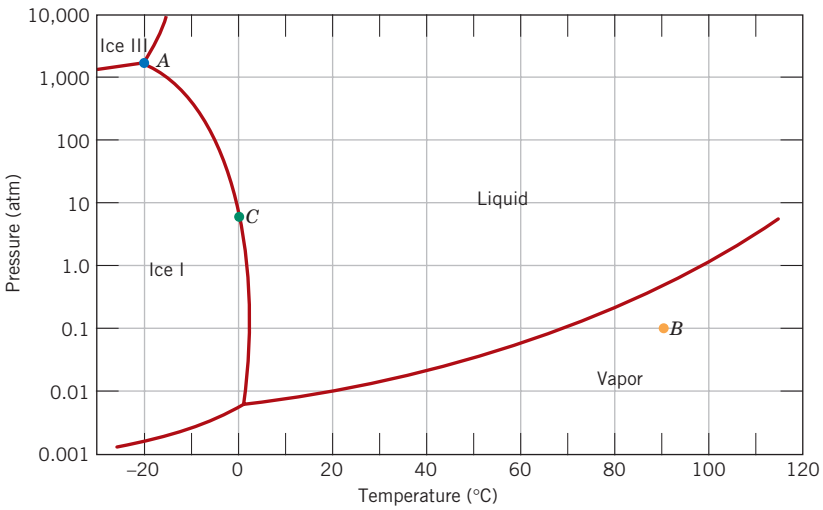

Figure 9.38 Logarithm pressure-versus-temperature phase diagram for H_2O.

- One congruent melting point occurs at 780°C and 51 wt% B–49 wt% A.
- A second congruent melting point occurs at 755°C and 67 wt% B–33 wt% A.
- The intermetallic compound AB exists at 51 wt% B–49 wt% A.
- The intermetallic compound AB_2 exists at 67 wt% B–33 wt% A.

The Gibbs Phase Rule

9.45 Figure 9.38 shows the pressure–temperature phase diagram for H_2O. Apply the Gibbs phase rule at points *A*, *B*, and *C*; that is, specify the number of degrees of freedom at each of the points—that is, the number of externally controllable variables that need be specified to completely define the system.

The Iron–Iron Carbide (Fe–Fe_3C) Phase Diagram

Development of Microstructure in Iron–Carbon Alloys

9.46 Compute the mass fractions of α-ferrite and cementite in pearlite.

9.47 **(a)** What is the distinction between hypoeutectoid and hypereutectoid steels?

(b) In a hypoeutectoid steel, both eutectoid and proeutectoid ferrite exist. Explain the difference between them. What will be the carbon concentration in each?

9.48 What is the carbon concentration of an iron–carbon alloy for which the fraction of total ferrite is 0.94?

9.49 What is the proeutectoid phase for an iron–carbon alloy in which the mass fractions of total ferrite and total cementite are 0.92 and 0.08, respectively? Why?

9.50 Consider 1.0 kg of austenite containing 1.15 wt% C, cooled to below 727°C (1341°F).

(a) What is the proeutectoid phase?

(b) How many kilograms each of total ferrite and cementite form?

(c) How many kilograms each of pearlite and the proeutectoid phase form?

(d) Schematically sketch and label the resulting microstructure.

9.51 Consider 2.5 kg of austenite containing 0.65 wt% C, cooled to below 727°C (1341°F).

(a) What is the proeutectoid phase?

(b) How many kilograms each of total ferrite and cementite form?

(c) How many kilograms each of pearlite and the proeutectoid phase form?

(d) Schematically sketch and label the resulting microstructure.

9.52 Compute the mass fractions of proeutectoid ferrite and pearlite that form in an iron–carbon alloy containing 0.25 wt% C.

9.53 The microstructure of an iron–carbon alloy consists of proeutectoid ferrite and pearlite; the mass fractions of these two microconstituents are 0.286 and 0.714, respectively. Determine the concentration of carbon in this alloy.

9.54 The mass fractions of total ferrite and total cementite in an iron–carbon alloy are 0.88 and 0.12, respectively. Is this a hypoeutectoid or hypereutectoid alloy? Why?

9.55 The microstructure of an iron–carbon alloy consists of proeutectoid ferrite and pearlite; the mass fractions of these microconstituents are 0.20 and 0.80, respectively. Determine the concentration of carbon in this alloy.

9.56 Consider 2.0 kg of a 99.6 wt% Fe–0.4 wt% C alloy that is cooled to a temperature just below the eutectoid.

(a) How many kilograms of proeutectoid ferrite form?

(b) How many kilograms of eutectoid ferrite form?

(c) How many kilograms of cementite form?

9.57 Compute the maximum mass fraction of proeutectoid cementite possible for a hypereutectoid iron–carbon alloy.

9.58 Is it possible to have an iron–carbon alloy for which the mass fractions of total ferrite and proeutectoid cementite are 0.846 and 0.049, respectively? Why or why not?

9.59 Is it possible to have an iron–carbon alloy for which the mass fractions of total cementite and pearlite are 0.039 and 0.417, respectively? Why or why not?

9.60 Compute the mass fraction of eutectoid ferrite in an iron–carbon alloy that contains 0.43 wt% C.

9.61 The mass fraction of *eutectoid* cementite in an iron–carbon alloy is 0.104. On the basis of this information, is it possible to determine the composition of the alloy? If so, what is its composition? If this is not possible, explain why.

9.62 The mass fraction of *eutectoid* ferrite in an iron–carbon alloy is 0.82. On the basis of this information, is it possible to determine the composition of the alloy? If so, what is its composition? If this is not possible, explain why.

9.63 For an iron–carbon alloy of composition 5 wt% C–95 wt% Fe, make schematic sketches of the microstructure that would be observed for conditions of very slow cooling at the following temperatures: 1175°C (2150°F), 1145°C (2095°F), and 700°C (1290°F). Label the phases and indicate their compositions (approximate).

9.64 Often, the properties of multiphase alloys may be approximated by the relationship

$$E\ (\text{alloy}) = E_\alpha V_\alpha + E_\beta V_\beta \qquad (9.24)$$

where E represents a specific property (modulus of elasticity, hardness, etc.), and V is the volume fraction. The subscripts α and β denote the existing phases or microconstituents. Employ this relationship to determine the approximate Brinell hardness of a 99.80 wt% Fe–0.20 wt% C alloy. Assume Brinell hardnesses of 80 and 280 for ferrite and pearlite, respectively, and that volume fractions may be approximated by mass fractions.

The Influence of Other Alloying Elements

9.65 A steel alloy contains 97.5 wt% Fe, 2.0 wt% Mo, and 0.5 wt% C.

(a) What is the eutectoid temperature of this alloy?

(b) What is the eutectoid composition?

(c) What is the proeutectoid phase?

Assume that there are no changes in the positions of other phase boundaries with the addition of Mo.

9.66 A steel alloy is known to contain 93.8 wt% Fe, 6.0 wt% Ni, and 0.2 wt% C.

(a) What is the approximate eutectoid temperature of this alloy?

(b) What is the proeutectoid phase when this alloy is cooled to a temperature just below the eutectoid?

(c) Compute the relative amounts of the proeutectoid phase and pearlite.

Assume that there are no alterations in the positions of other phase boundaries with the addition of Ni.